Bottomonium suppression in the QGP
From EFTs to non-unitary quantum evolution

Michael Strickland

Kent State University
Kent, OH USA

N. Brambilla, M.-A. Escobedo, M.S., A. Vairo,
P. Vander Griend, and J.H. Weber, arXiv:2012.01240 and forthcoming

Arizona State University Online Theoretical Physics Colloquium
May 5, 2021

KENT STATE UNIVERSITY   U.S. DEPARTMENT OF ENERGY   TUM Global   Ohio Supercomputer Center An OH·TECH Consortium Member

Bottomonium Suppression

- In a high temperature quark-gluon plasma we expect **weaker color binding** (Debye screening + asymptotic freedom)

E. V. Shuryak, Phys. Rept. 61, 71–158 (1980)
T. Matsui, and H. Satz, Phys. Lett. B178, 416 (1986)
F. Karsch, M. T. Mehr, and H. Satz, Z. Phys. C37, 617 (1988)

- Also, high energy plasma particles which slam into the bound states cause them to have shorter lifetimes → **larger spectral widths**

TUMQCD Collaboration, 1804.10600

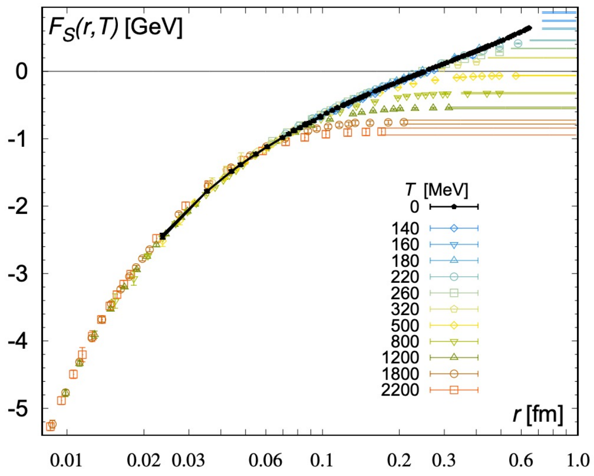

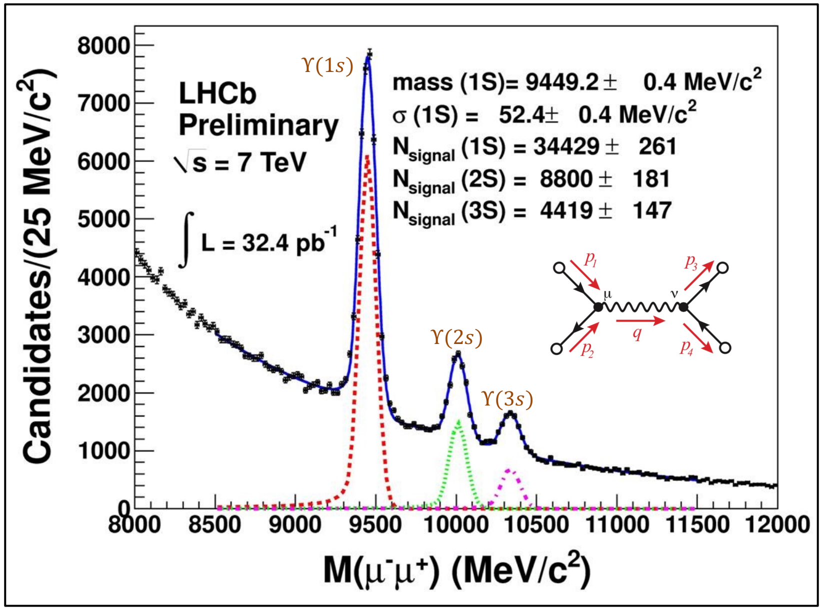

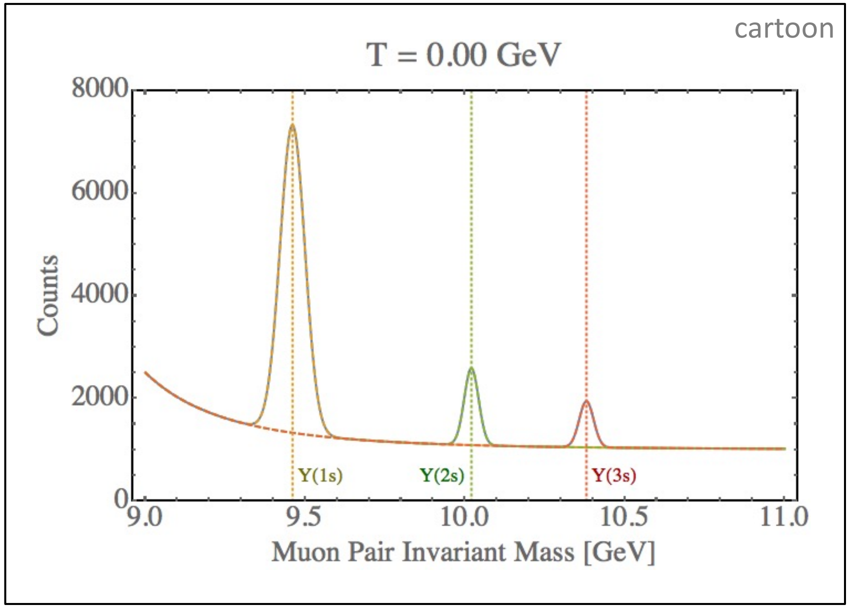

Bottomonium Suppression

- In a high temperature quark-gluon plasma we expect **weaker color binding** (Debye screening + asymptotic freedom)

E. V. Shuryak, Phys. Rept. 61, 71–158 (1980)
T. Matsui, and H. Satz, Phys. Lett. B178, 416 (1986)
F. Karsch, M. T. Mehr, and H. Satz, Z. Phys. C37, 617 (1988)

- Also, high energy plasma particles which slam into the bound states cause them to have shorter lifetimes → **larger spectral widths**

TUMQCD Collaboration, 1804.10600

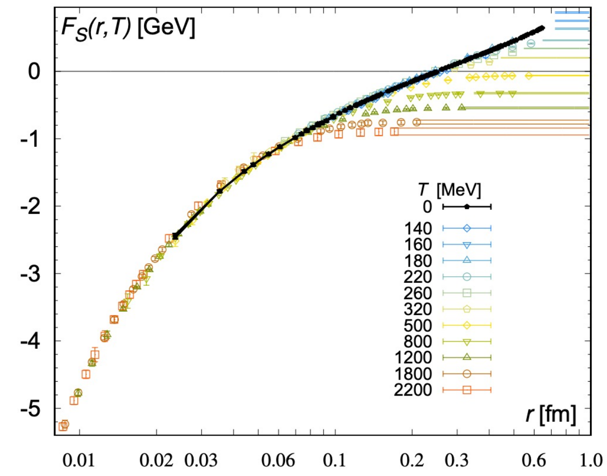

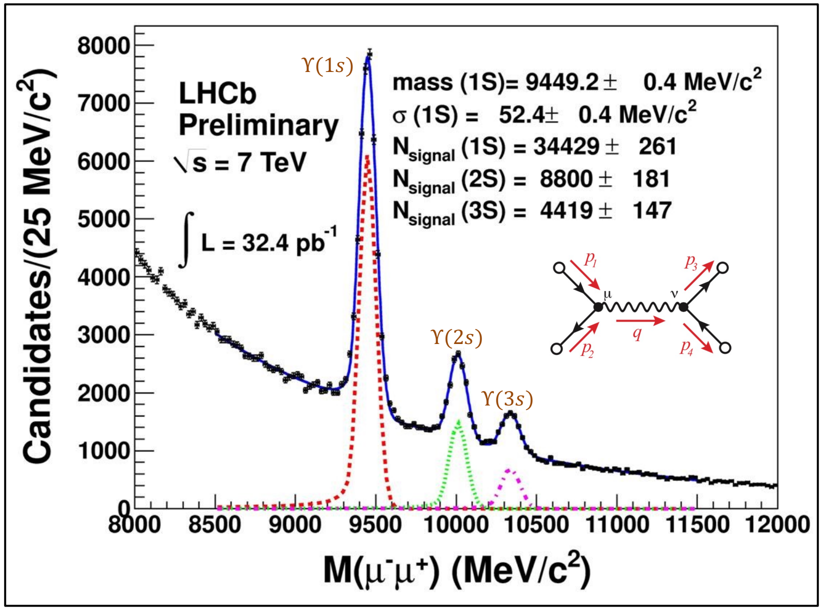

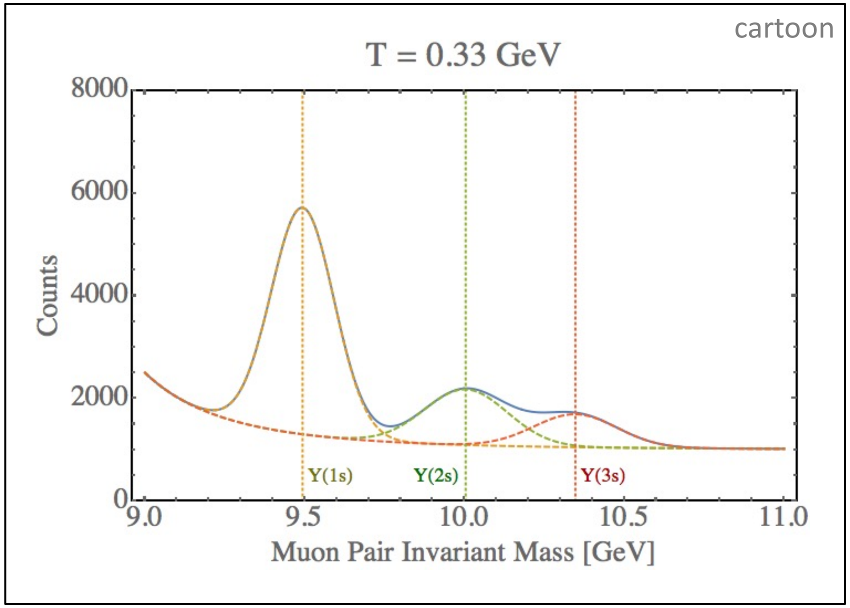

Bottomonium Suppression

- In a high temperature quark-gluon plasma we expect **weaker color binding** (Debye screening + asymptotic freedom)

E. V. Shuryak, Phys. Rept. 61, 71–158 (1980)
T. Matsui, and H. Satz, Phys. Lett. B178, 416 (1986)
F. Karsch, M. T. Mehr, and H. Satz, Z. Phys. C37, 617 (1988)

- Also, high energy plasma particles which slam into the bound states cause them to have shorter lifetimes → **larger spectral widths**

TUMQCD Collaboration, 1804.10600

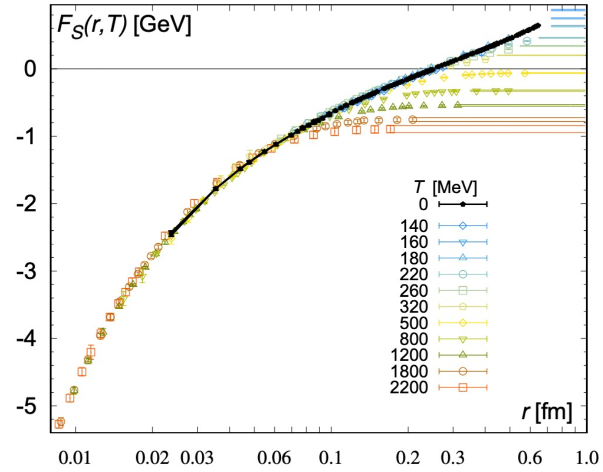

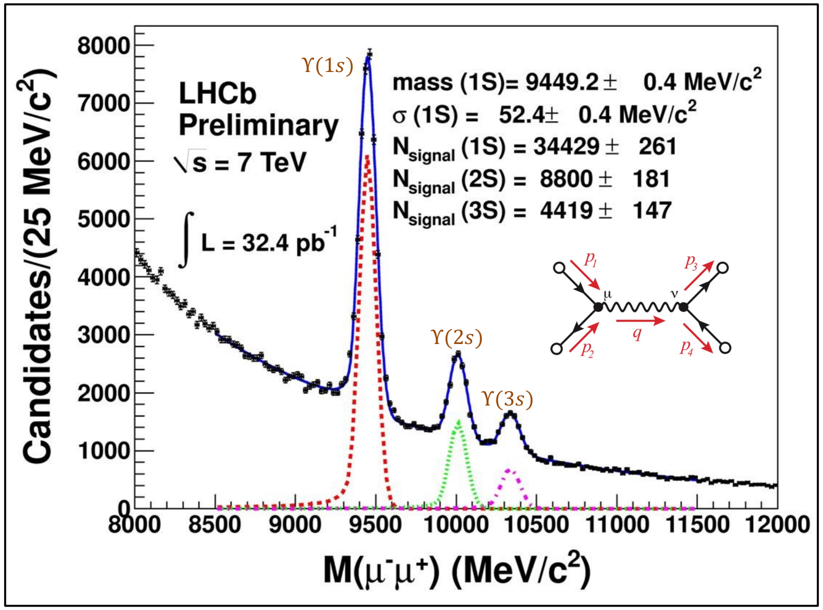

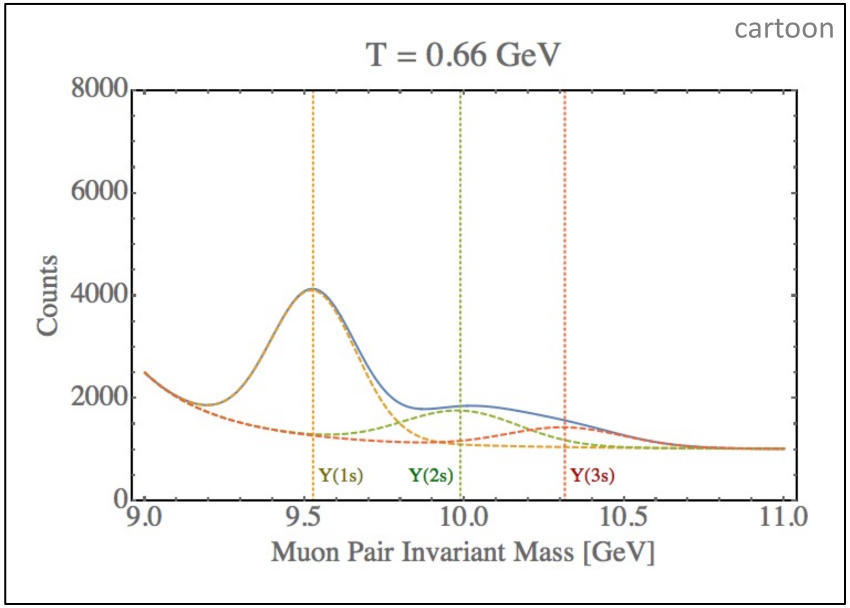

Bottomonium Suppression

- In a high temperature quark-gluon plasma we expect **weaker color binding** (Debye screening + asymptotic freedom)

E. V. Shuryak, Phys. Rept. 61, 71–158 (1980)
T. Matsui, and H. Satz, Phys. Lett. B178, 416 (1986)
F. Karsch, M. T. Mehr, and H. Satz, Z. Phys. C37, 617 (1988)

- Also, high energy plasma particles which slam into the bound states cause them to have shorter lifetimes → **larger spectral widths**

TUMQCD Collaboration, 1804.10600

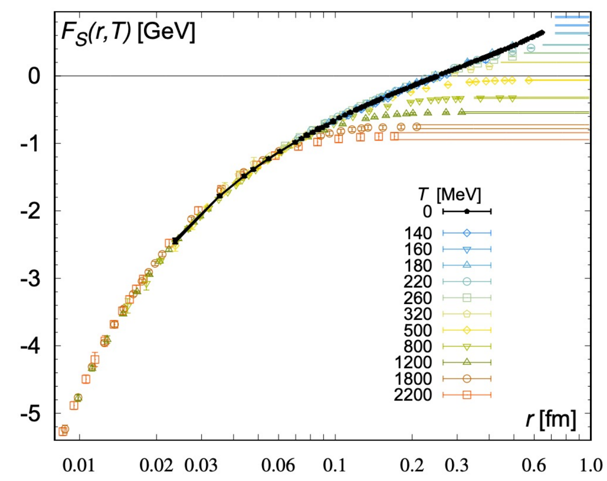

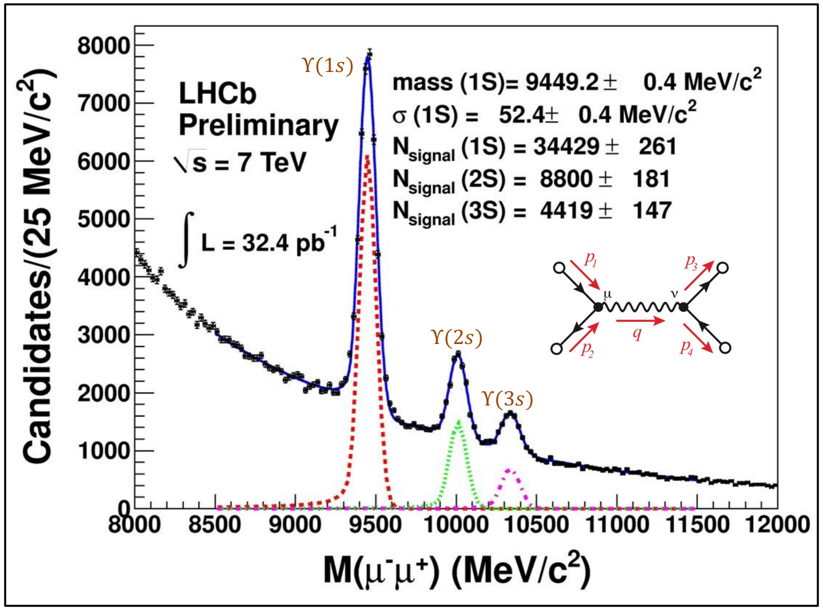

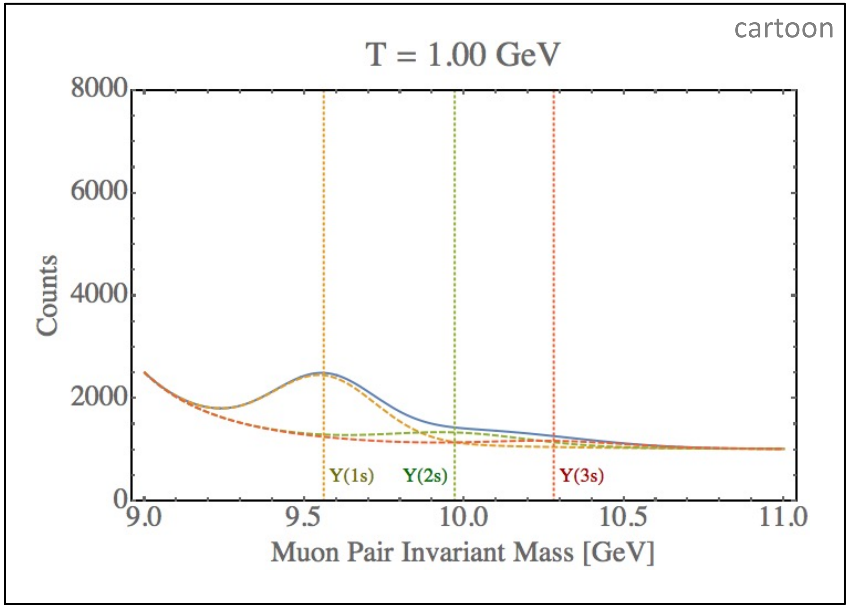

Experimental data – 5.02 TeV Dimuon Spectra

The **CMS, ALICE,** and **ATLAS** experiments have measured bottomonium production in both pp and Pb-Pb collisions. Here I show CMS results.

pp

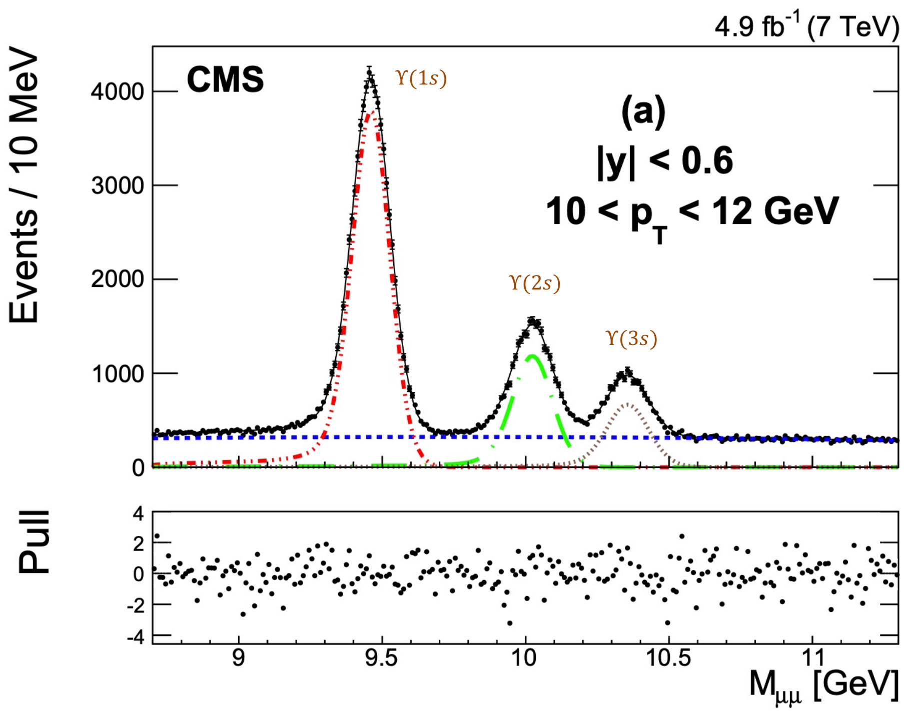

PbPb

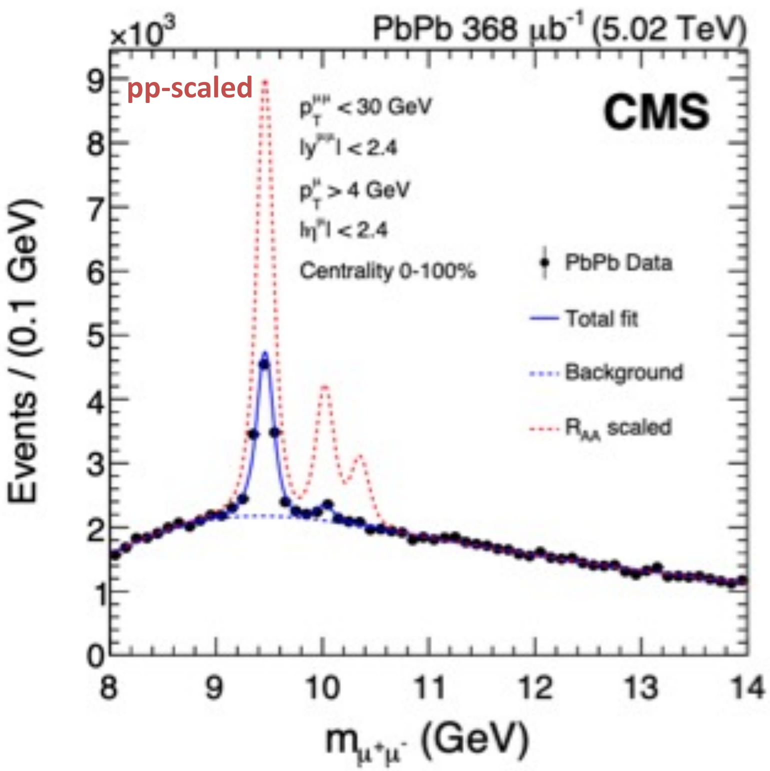

Experimental data – 5.02 TeV Dimuon Spectra

The **CMS, ALICE,** and **ATLAS** experiments have measured bottomonium production in both pp and Pb-Pb collisions. Here I show CMS results.

pPb

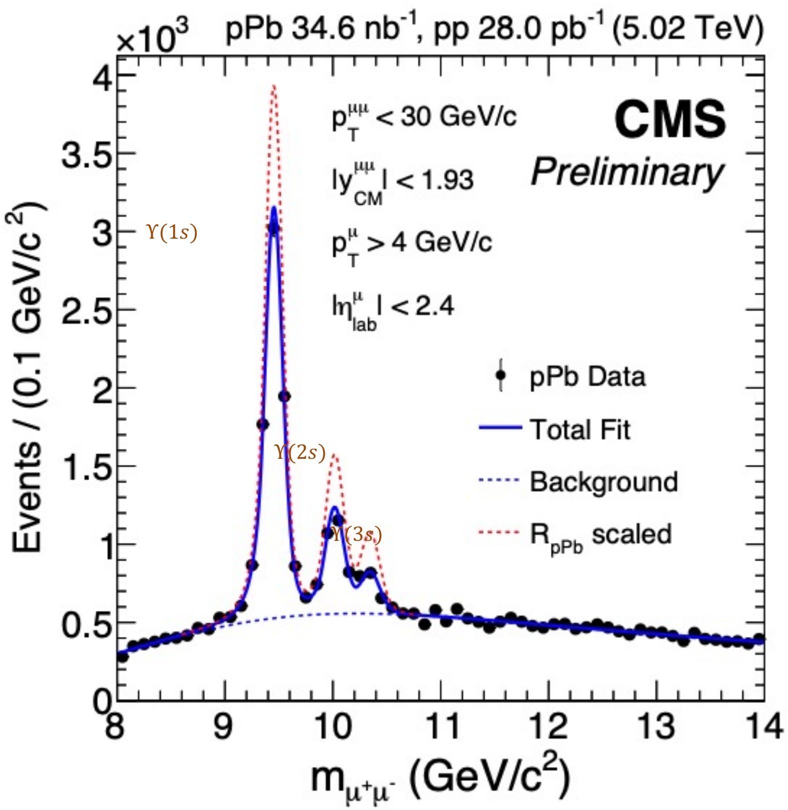

PbPb

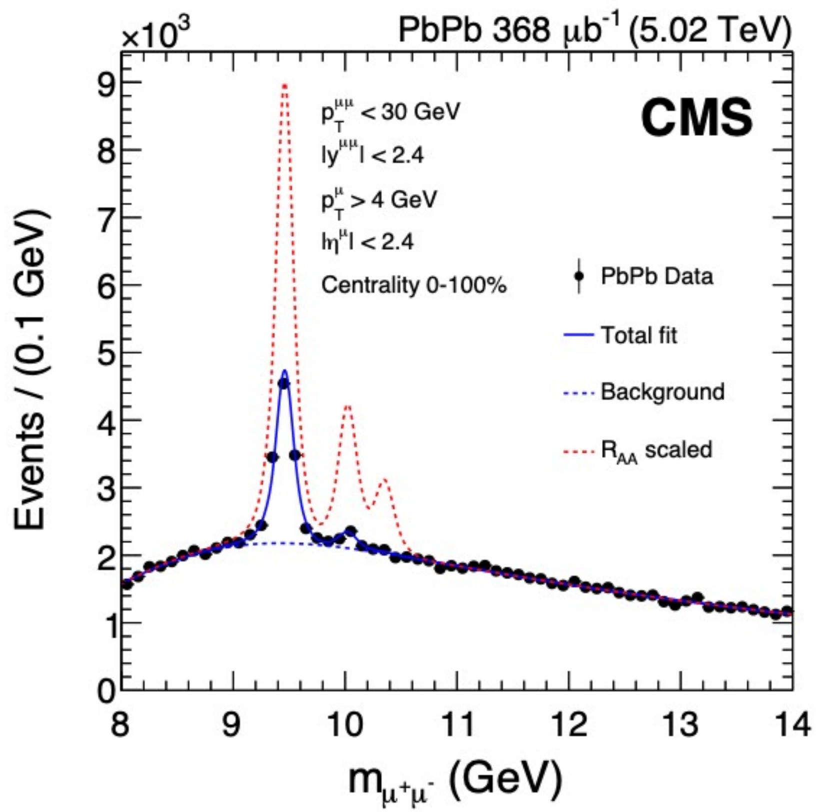

Why bottomonia in AA?

- Can trust heavy quark effective theory more.
- Cold nuclear matter (CNM) effects in AA decrease with increasing quark mass.
- The masses of bottomonia (m_{Υ} ~ 10 GeV) are much higher than the temperature (T < 1 GeV) generated in HICs → bottomonia production dominated by initial hard scatterings.

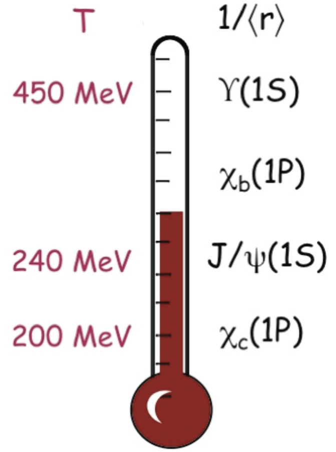

A. Mocsy, P. Petreczky, and MS, 1302.2180

- Since bottom quarks and anti-quarks are relatively rare in LHC HICs, the probability for regeneration of bottomonia through statistical recombination is much smaller than for charm quarks. [see e.g. E. Emerick, X. Zhao, and R. Rapp, arXiv:1111.6537]

Conceptual problem

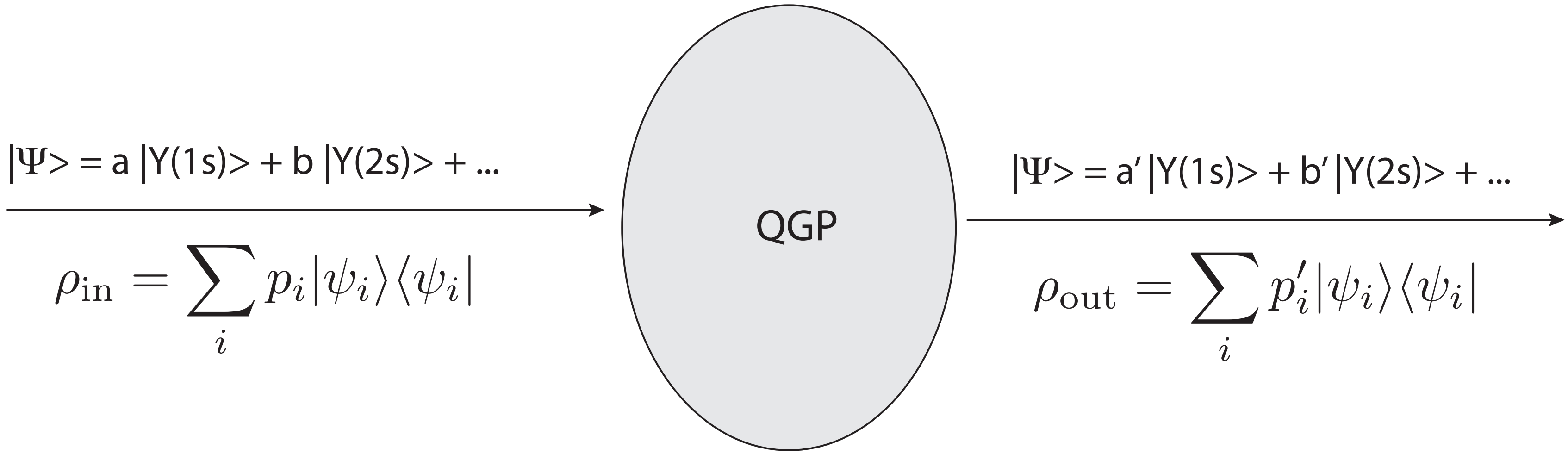

- Bottomonium states have a large binding energy and are produced locally (hard processes) at early times in hard collisions (t < 1 fm/c).
- They then propagate through the plasma and interact with the medium.
- Bound states can break up and potentially re-form due to in-medium transitions induced by in-medium gluon absorption and emission.

Heuristic understanding – Noisy QM

- Heavy quark bound states have an in-medium potential with both real and imaginary parts. This is related to the large in-medium width.
- How can we understand the emergence of the imaginary part in a simple manner before leaping into open quantum systems + pNRQCD?
- **Consider a non-relativistic bound state subject to a noisy potential**

$$H(\mathbf{r},t) = -\frac{\nabla_{\mathbf{r}}^2}{M} + V(\mathbf{r}) + \Theta(\mathbf{r},t) \qquad \Theta(\mathbf{r},t) = \theta\left(\mathbf{R}+\frac{\mathbf{r}}{2},t\right) - \theta\left(\mathbf{R}-\frac{\mathbf{r}}{2},t\right)$$

Noise due to environment (assumed here to be color neutral).

- Noise has zero mean, is uncorrelated in time, and has a spatial correlation function $D(\boldsymbol{r})$

$$\langle\theta(\mathbf{x},t)\rangle = 0 \qquad \langle\theta(\mathbf{x},t)\theta(\mathbf{x}',t')\rangle = D(\mathbf{x}-\mathbf{x}')\delta(t-t')$$

Note: The treatment presented here does not include possibility of color-charged noise, more on this coming…

Heuristic understanding – Noisy QM

- Expanding the time evolution operator up to $O(\Delta t^{3/2})$

$$e^{-i\Delta t\, H(\mathbf{r},t)} \simeq 1 - i\Delta t\, H(\mathbf{r},t) - \frac{1}{2}\{\Delta t\, H(\mathbf{r},t)\}^2 + \ldots$$

$$\approx 1 - i\Delta t\left[H(\mathbf{r},t) - \frac{i}{2}\Delta t\left\{\theta(\mathbf{x},t)^2 + \theta(\mathbf{x}',t)^2 - 2\,\theta(\mathbf{x},t)\theta(\mathbf{x}',t)\right\}\right]$$

- Now construct an effective Hamiltonian that is averaged over the noise

$$\langle \mathrm{H_{eff}}(\mathbf{r},t)\rangle \simeq H(\mathbf{r},t) - \frac{i}{2}\Delta t\left\{\langle\theta(\mathbf{x},t)^2\rangle + \langle\theta(\mathbf{x}',t)^2\rangle - 2\,\langle\theta(\mathbf{x},t)\theta(\mathbf{x}',t)\rangle\right\}$$

Imaginary part of the potential

$$\langle \mathrm{H_{eff}}(\mathbf{r},t)\rangle = -\frac{\nabla^2_{\mathbf{r}}}{M} + V(\mathbf{r}) - i\left\{D(\mathbf{0}) - D(\mathbf{r})\right\}$$

$$\Im[V(r)] = D(\mathbf{r}) - D(\mathbf{0})$$

Imaginary part emerges through interference of wave function with itself when summing over environmental noise.

Open quantum system (OQS) approach

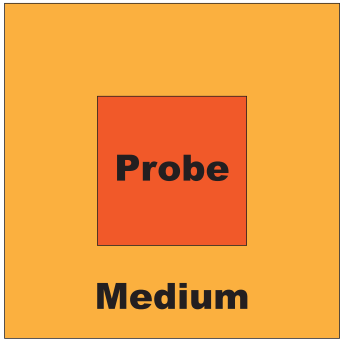

Probe = heavy-quarkonium state

Medium = light quarks and gluons that comprise the QGP

- Can treat heavy quarkonium states propagating through QGP using an open quantum system approach

$$H_{\rm tot} = H_{\rm probe} \otimes I_{\rm medium} + I_{\rm probe} \otimes H_{\rm medium} + H_{\rm int}$$

- Total density matrix

$$\rho_{\rm tot} = \sum_k \frac{1}{Z_{\rm tot}} e^{-E_k/T} |E_k\rangle\langle E_k| \longrightarrow \frac{d}{dt}\rho_{\rm tot} = -i[H_{\rm tot}, \rho_{\rm tot}]$$

- Reduced density matrix

$$\rho_{\rm probe} = {\rm Tr}_{\rm medium}[\rho_{\rm tot}] \longrightarrow$$ **Evolution equation?**

The Lindblad equation

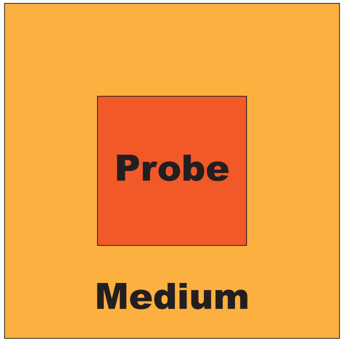

Probe = heavy-quarkonium state

Medium = light quarks and gluons that comprise the QGP

- Separation of time scales
  - Medium relaxation time scale $\langle \hat{O}_{\rm M}(t)\hat{O}_{\rm M}(0)\rangle \sim e^{-t/t_{\rm M}}$
  - Intrinsic probe time scale $t_P \sim \dfrac{1}{\omega_i - \omega_j}$
  - Probe relaxation time scale $\langle p(t)\rangle \sim e^{-t/t_{\rm rel}}$

Lindblad equation

$t_{\rm rel}\,,\, t_{\rm P} \gg t_{\rm M}$ →

$$\frac{d\rho_{\rm probe}}{dt} = -i[H_{\rm probe}, \rho_{\rm probe}] + \sum_n \left(C_n\, \rho_{\rm probe}\, C_n^\dagger - \frac{1}{2}\{C_n^\dagger C_n, \rho_{\rm probe}\} \right)$$

- Trace preserving
- Completely positive
- In general, non-unitary evolution

G. Lindblad, Commun. Math. Phys. 48 (1976) 119
V. Gorini, et.al. J. Math. Phys. 17 (1976) 821

Bottomonium scales

- The mass scale is perturbative: $m_b \sim 5$ GeV
- The system is non-relativistic ($v \ll 1$), with $v_b \sim 0.1$.
- $\Delta_n E \sim m v^2$ and $\Delta_{\text{fs}} E \sim m v^4$

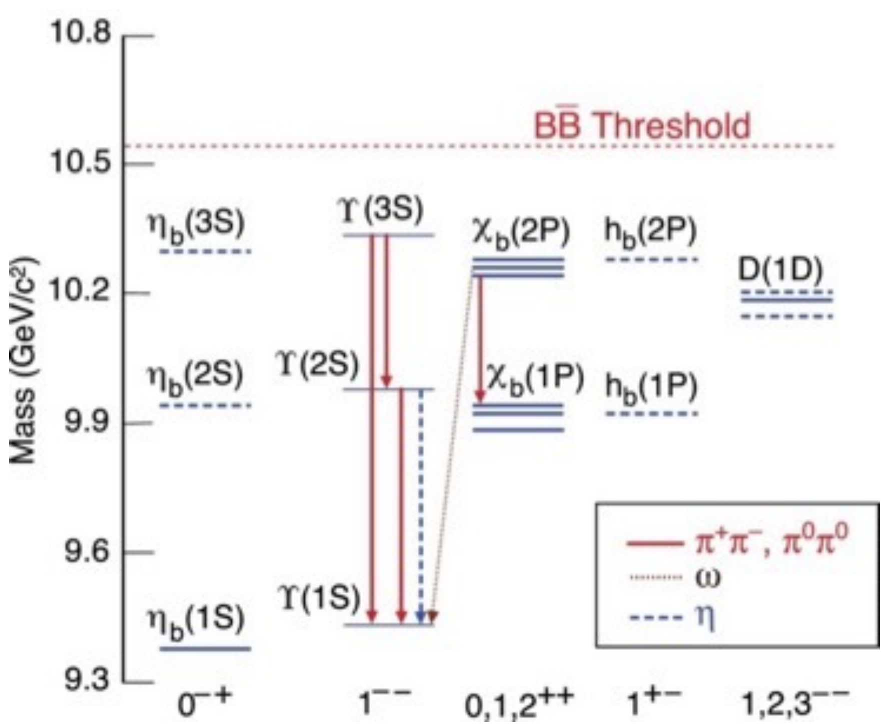

Results of a non-relativistic potential model

State	Name	Exp. [92]	Model	Rel. Err.
1^1S_0	$\eta_b(1S)$	9.398 GeV	9.398 GeV	0.001%
1^3S_1	$\Upsilon(1S)$	9.461 GeV	9.461 GeV	0.004%
1^3P_0	$\chi_{b0}(1P)$	9.859 GeV	9.869 GeV	0.21%
1^3P_1	$\chi_{b1}(1P)$	9.893 GeV		
1^3P_2	$\chi_{b2}(1P)$	9.912 GeV		
1^1P_1	$h_b(1P)$	9.899 GeV		
2^1S_0	$\eta_b(2S)$	9.999 GeV	9.977 GeV	0.22%
2^3S_1	$\Upsilon(2S)$	10.002 GeV	9.999 GeV	0.03%
2^3P_0	$\chi_{b0}(2P)$	10.232 GeV	10.246 GeV	0.05%
2^3P_1	$\chi_{b1}(2P)$	10.255 GeV		
2^3P_2	$\chi_{b2}(2P)$	10.269 GeV		
2^1P_1	$h_b(2P)$	-		
3^1S_0	$\eta_b(3S)$	-	10.344 GeV	-
3^3S_1	$\Upsilon(3S)$	10.355 GeV	10.358 GeV	0.03%

J. Alford and MS, 1309.3003

Non-Relativistic QCD (NRQCD)

Caswell and Lepage (1986), Bodwin, Braaten and Lepage (1994)

$$\mathcal{L}_{NRQCD} = \mathcal{L}_g + \mathcal{L}_q + \mathcal{L}_\psi + \mathcal{L}_\chi + \mathcal{L}_{\psi\chi}$$

$$\mathcal{L}_g = -\frac{1}{4} F^a_{\mu\nu} F^{\mu\nu a} + \frac{d_2}{m_Q^2} F^a_{\mu\nu} D^2 F^{\mu\nu a} + d_g^3 \frac{1}{m_Q^2} g f_{abc} F^a_{\mu\nu} F^{\mu b}_{\alpha} F^{\nu\alpha c}$$

$$\mathcal{L}_\psi = \psi^\dagger \left(iD_0 + c_2 \frac{\mathrm{D}^2}{2m_Q} + c_4 \frac{\mathrm{D}^4}{8m_Q^3} + c_F g \frac{\sigma \mathrm{B}}{2m_Q} + c_D g \frac{\mathrm{DE}-\mathrm{ED}}{8m_Q^2} \right.$$
$$\left. + i c_S g \frac{\sigma(\mathrm{D}\times\mathrm{E} - \mathrm{E}\times\mathrm{D})}{8m_Q^2} \right) \psi$$

$$\mathcal{L}_\chi = c.c \text{ of } \mathcal{L}_\psi$$

$$\mathcal{L}_{\psi\chi} = \frac{f_1(^1S_0)}{m_Q^2} \psi^\dagger \chi \chi^\dagger \psi + \frac{f_1(^3S_1)}{m_Q^2} \psi^\dagger \sigma \chi \chi^\dagger \sigma \psi + \frac{f_8(^1S_0)}{m_Q^2} \psi^\dagger T^a \chi \chi^\dagger T^a \psi$$
$$+ \frac{f_8(^3S_1)}{m_Q^2} \psi^\dagger T^a \sigma \chi \chi^\dagger T^a \sigma \psi$$

- **Integrating out the scale m can be done perturbatively** and is not affected by the presence of the medium since $m \gg \Lambda_{QCD}, T$.
- **Hard gluons**, with energy and momentum of order m.
- **Soft gluons**, with energy and momentum of order mv.
- **Potential gluons**, with energy of order mv^2 and momentum of order mv.
- **Ultrasoft gluons**, with both energy and momentum of order mv^2

NRQCD → Potential NRQCD (pNRQCD)

Pineda and Soto, '97; Brambilla, Pineda, Soto, and Vairo '99, '00, '03

Degrees of freedom at scale $\frac{1}{r} = mv$ are integrated out

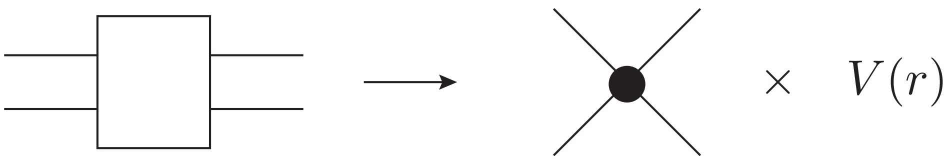

Power counting

$$r \sim \frac{1}{mv} \qquad t, R \sim \frac{1}{mv^2}, \frac{1}{\Lambda_{\rm QCD}}$$

Gauge fields are multiple expanded

$$A(r, R, t) = A(R, t) + \mathbf{r} \cdot \nabla A(R, t) + \ldots$$

Non-analytic behavior in r → matching coefficients V

- Resulting degrees of freedom are singlet and octet states (see Lagrangian on next slide).
- Allows to obtain manifestly gauge-invariant results.
- Easier connection lattice QCD.
- If $1/r \gg T$ we can use this as a starting point.
- In other cases, the matching between NRQCD and pNRQCD will be modified.

NRQCD → Potential NRQCD (pNRQCD)

Pineda and Soto, ‘97; Brambilla, Pineda, Soto, and Vairo ‘99, ‘00, ‘03

$$\mathcal{L} = -\frac{1}{4}F^a_{\mu\nu}F^{\mu\nu,a} + \mathrm{Tr}\left\{S^\dagger\left(i\partial_0 - \frac{\mathbf{p}^2}{m} - V_s\right)S + O^\dagger\left(i\partial_0 - \frac{\mathbf{p}^2}{m} - V_o\right)O\right\}$$

$$+V_A \mathrm{Tr}\left\{O^\dagger\,\mathbf{r}\cdot g\mathbf{E}\,S + S^\dagger\,\mathbf{r}\cdot g\mathbf{E}\,O\right\} \rightarrow$$

$O^\dagger \mathbf{r}\cdot g\mathbf{E}\,\mathrm{S}$

$$+\frac{V_B}{2}\mathrm{Tr}\left\{O^\dagger\,\mathbf{r}\cdot g\mathbf{E}\,O + O^\dagger O\,\mathbf{r}\cdot g\mathbf{E}\right\} \rightarrow$$

$O^\dagger\{\mathbf{r}\cdot g\mathbf{E},\mathrm{O}\}$

Singlet and octet potentials

$$V_s(r) = -C_F\frac{\alpha_s}{r}$$

$$V_o(r) = \frac{\alpha_s}{2N_c r}$$

- Based on this Lagrangian, we can perform first-principles calculations.
- Right figure shows diagrams contributing to singlet and octet self-energies.
- These enter into the calculation of Lindblad/collapse/jump operators.

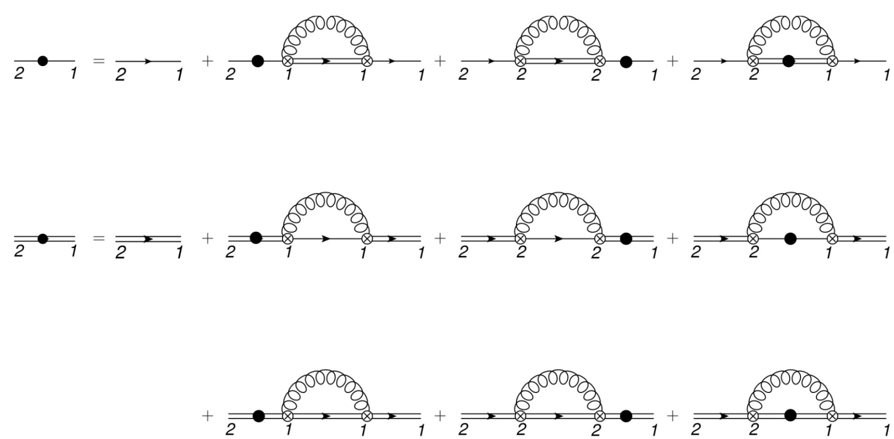

OQS + pNRQCD → Lindblad equation

- What are the relevant scales?
  - Temperature T
  - Bound state mass $m \gg T$
  - Bound state size $r \sim mv \sim a_0$ (Bohr radius)
  - Debye mass m_D
  - Binding energy $E \sim mv^2$

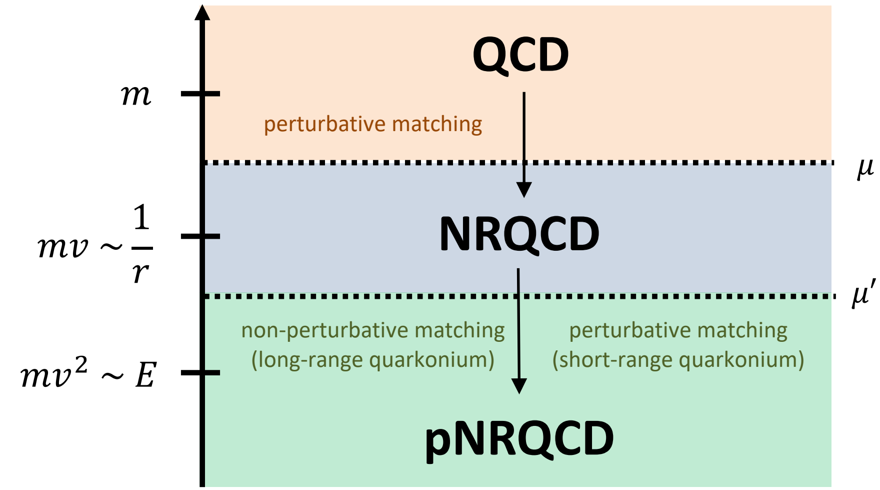

- Separation of time scales
  - Medium relaxation time scale $\quad \langle \hat{O}_{\rm M}(t)\hat{O}_{\rm M}(0)\rangle \sim e^{-t/t_{\rm M}} \rightarrow \frac{1}{T}$
  - Intrinsic probe time scale $\quad t_P \sim \frac{1}{\omega_i - \omega_j} \rightarrow \frac{1}{E}$
  - Probe relaxation time scale $\quad \langle p(t)\rangle \sim e^{-t/t_{\rm rel}} \rightarrow \frac{1}{\text{self-energy}} \sim \frac{1}{\alpha_s a_0^2 \Lambda^3} \qquad \Lambda = T, E$

$$1/r \gg T \sim m_D \gg E \quad \xrightarrow[t_{\rm rel}\,,\, t_{\rm P} \gg t_{\rm M}]{} \quad \boxed{\frac{d\rho_{\rm probe}}{dt} = -i[H_{\rm probe}, \rho_{\rm probe}] + \sum_n \left(C_n\, \rho_{\rm probe}\, C_n^\dagger - \frac{1}{2}\{C_n^\dagger C_n, \rho_{\rm probe}\}\right)}$$

Lindblad equation

N. Brambilla, M. A. Escobedo, J. Soto and A. Vairo, 1612.07248, 1711.04515

OQS + pNRQCD – Relevant scaling

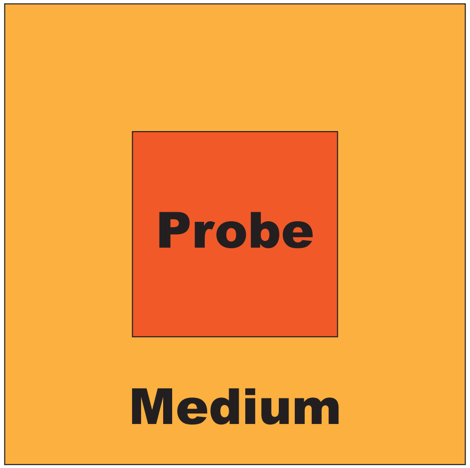

What are the relevant scales?

- Temperature T
- Bound state mass $m \gg T$
- Bound state size $r \sim mv \sim a_0$
- Debye mass m_D
- Binding energy $E \sim mv^2$

Medium

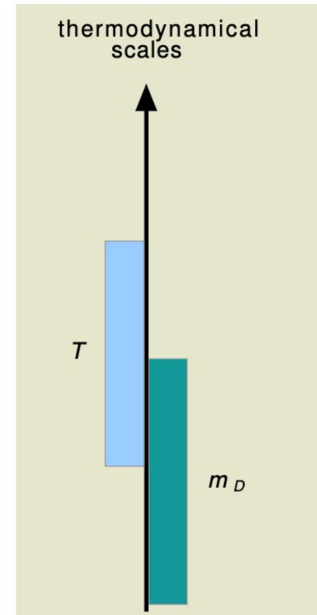

Strongly-coupled QGP

$$1/r \gg T \sim m_D \gg E$$

Lindblad equation

$$\rho_{\rm probe} = {\rm Tr}_{\rm medium}[\rho_{\rm tot}] \xrightarrow[1/r \gg T \sim m_D \gg E]{} \quad \frac{d\rho_{\rm probe}}{dt} = -i[H_{\rm probe}, \rho_{\rm probe}] + \sum_n \left(C_n\, \rho_{\rm probe}\, C_n^\dagger - \frac{1}{2}\{C_n^\dagger C_n, \rho_{\rm probe}\} \right)$$

N. Brambilla, M. A. Escobedo, J. Soto and A. Vairo, 1612.07248, 1711.04515

OQS + pNRQCD – Lindblad reorganization

$$\frac{d\rho_{\rm probe}}{dt} = -i[H_{\rm probe}, \rho_{\rm probe}] + \sum_n \left(C_n \, \rho_{\rm probe} \, C_n^\dagger - \frac{1}{2}\{C_n^\dagger C_n, \rho_{\rm probe}\} \right)$$

- $H_{\rm probe}$ is a Hermitian operator (includes singlet and octet states)
- C_n are the **collapse (or jump) operators** (connect different internal states)
- Partial and **total decay widths** are

$$\Gamma_n = C_n^\dagger C_n \qquad \Gamma = \sum_n \Gamma_n$$

- Can reorganize Lindblad equation by defining

$$H_{\rm eff} = H_{\rm probe} - \frac{i}{2}\Gamma$$

← **Non-Hermitian effective Hamiltonian**

⟶

$$\frac{d\rho_{\rm probe}}{dt} = -iH_{\rm eff}\rho_{\rm probe} + i\rho_{\rm probe}H_{\rm eff}^\dagger + \sum_n C_n \, \rho_{\rm probe} \, C_n^\dagger$$

OQS+pNRQCD Hamiltonian and collapse operators

N. Brambilla, M. A. Escobedo, J. Soto and A. Vairo, 1612.07248, 1711.04515

$$\frac{d\rho_{\rm probe}}{dt} = -iH_{\rm eff}\rho_{\rm probe} + i\rho_{\rm probe}H_{\rm eff}^\dagger + \sum_n C_n\,\rho_{\rm probe}\,C_n^\dagger$$

$$\rho = \begin{pmatrix} \rho_s & 0 \\ 0 & \rho_o \end{pmatrix}$$

$$H_{\rm probe} = \begin{pmatrix} h_s & 0 \\ 0 & h_o \end{pmatrix} + \frac{r^2}{2}\gamma \begin{pmatrix} 1 & 0 \\ 0 & \frac{N_c^2-2}{2(N_c^2-1)} \end{pmatrix}$$

mass shift

$$C_i^0 = \sqrt{\frac{\kappa}{N_c^2-1}}\, r^i \begin{pmatrix} 0 & 1 \\ \sqrt{N_c^2-1} & 0 \end{pmatrix},$$

$$C_i^1 = \sqrt{\frac{(N_c^2-4)\kappa}{2(N_c^2-1)}}\, r^i \begin{pmatrix} 0 & 0 \\ 0 & 1 \end{pmatrix}.$$

$$\Gamma = \kappa r^i \begin{pmatrix} 1 & 0 \\ 0 & \frac{N_c^2-2}{2(N_c^2-1)} \end{pmatrix} r^i$$

Total width → Im[V]

$$H_{\rm eff} = H_{\rm probe} - \frac{i}{2}\Gamma$$

Six collapse operators cover

- singlet → octet,
- octet → singlet
- octet → octet

$$\gamma \equiv \frac{g^2}{6\,N_c}\,{\rm Im}\int_{-\infty}^{+\infty} ds\,\langle T\,E^{a,i}(s,\mathbf{0})E^{a,i}(0,\mathbf{0})\rangle$$

$$\kappa \equiv \frac{g^2}{6\,N_c}\,{\rm Re}\int_{-\infty}^{+\infty} ds\,\langle T\,E^{a,i}(s,\mathbf{0})E^{a,i}(0,\mathbf{0})\rangle$$

OQS+pNRQCD Hamiltonian and collapse operators

N. Brambilla, M. A. Escobedo, J. Soto and A. Vairo, 1612.07248, 1711.04515

$$\frac{d\rho_{\rm probe}}{dt} = -iH_{\rm eff}\rho_{\rm probe} + i\rho_{\rm probe}H^\dagger_{\rm eff} + \sum_n C_n\,\rho_{\rm probe}\,C^\dagger_n$$

$$\rho = \begin{pmatrix} \rho_s & 0 \\ 0 & \rho_o \end{pmatrix}$$

$$C_i^0 = \sqrt{\frac{\kappa}{N_c^2-1}}\, r^i \begin{pmatrix} 0 & 1 \\ \sqrt{N_c^2-1} & 0 \end{pmatrix},$$

$$C_i^1 = \sqrt{\frac{(N_c^2-4)\kappa}{2(N_c^2-1)}}\, r^i \begin{pmatrix} 0 & 0 \\ 0 & 1 \end{pmatrix}.$$

Six collapse operators cover

- singlet → octet,
- octet → singlet
- octet → octet

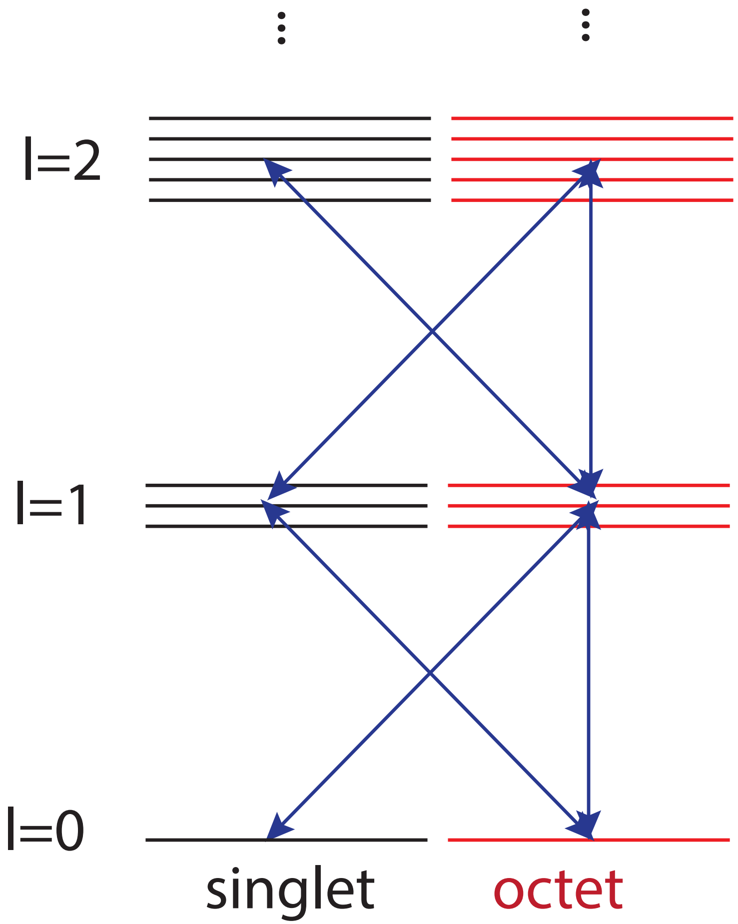

OQS+pNRQCD Hamiltonian and collapse operators

N. Brambilla, M. A. Escobedo, J. Soto and A. Vairo, 1612.07248, 1711.04515

$$\frac{d\rho_{\rm probe}}{dt} = -iH_{\rm eff}\rho_{\rm probe} + i\rho_{\rm probe}H_{\rm eff}^\dagger + \sum_n C_n\,\rho_{\rm probe}\,C_n^\dagger$$

$$\rho = \begin{pmatrix} \rho_s & 0 \\ 0 & \rho_o \end{pmatrix}$$

$$H_{\rm probe} = \begin{pmatrix} h_s & 0 \\ 0 & h_o \end{pmatrix} + \frac{r^2}{2}\gamma \begin{pmatrix} 1 & 0 \\ 0 & \frac{N_c^2-2}{2(N_c^2-1)} \end{pmatrix}$$

$$C_i^0 = \sqrt{\frac{\kappa}{N_c^2-1}}\,r^i \begin{pmatrix} 0 & 1 \\ \sqrt{N_c^2-1} & 0 \end{pmatrix},$$

$$C_i^1 = \sqrt{\frac{(N_c^2-4)\kappa}{2(N_c^2-1)}}\,r^i \begin{pmatrix} 0 & 0 \\ 0 & 1 \end{pmatrix}.$$

$$\Gamma = \kappa r^i \begin{pmatrix} 1 & 0 \\ 0 & \frac{N_c^2-2}{2(N_c^2-1)} \end{pmatrix} r^i$$

Six collapse operators cover

- singlet → octet,
- octet → singlet
- octet → octet

$$\gamma \equiv \frac{g^2}{6\,N_c}\,{\rm Im}\int_{-\infty}^{+\infty} ds\,\langle T\,E^{a,i}(s,\mathbf{0})E^{a,i}(0,\mathbf{0})\rangle$$

$$\kappa \equiv \frac{g^2}{6\,N_c}\,{\rm Re}\int_{-\infty}^{+\infty} ds\,\langle T\,E^{a,i}(s,\mathbf{0})E^{a,i}(0,\mathbf{0})\rangle$$

Values of $\hat{\kappa}$ and $\hat{\gamma}$ used

- We used NLO fits to recent lattice measurements of the heavy quark transport coefficient $\hat{\kappa} \equiv \kappa/T^3$.
  - N. Brambilla, V. Leino, P. Petreczky, and A. Vairo, 2007.10078

- The value of $\hat{\gamma} \equiv \gamma/T^3$ is less constrained, we vary it in the range -3.5 < $\hat{\gamma}$ < 0.
  - N. Brambilla, M. A. Escobedo, J. Soto and A. Vairo, 1612.07248.
  - N. Brambilla, M. A. Escobedo, J. Soto and A. Vairo, 1711.04515.
  - N. Brambilla, M. A. Escobedo, A. Vairo and P. Vander Griend, 1903.08063.

N. Brambilla, V. Leino, P. Petreczky, and A. Vairo, 2007.10078

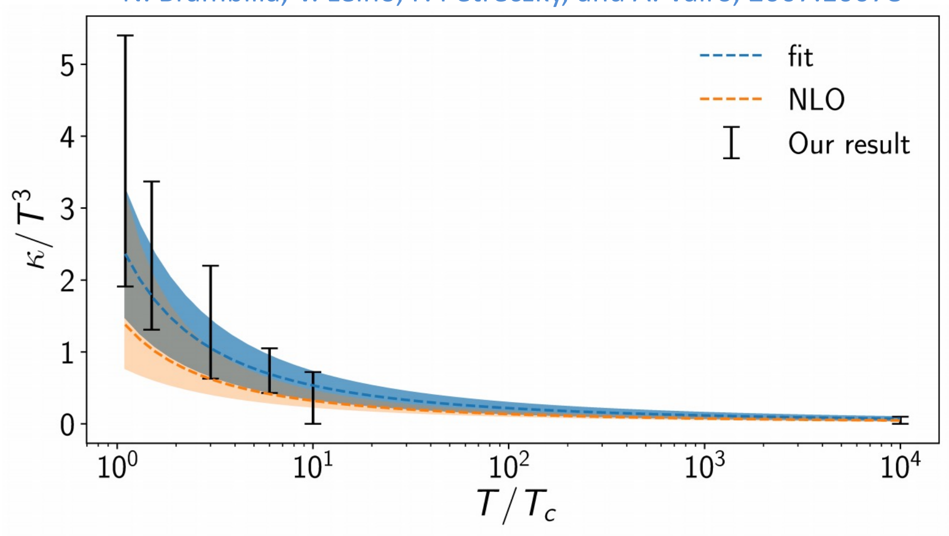

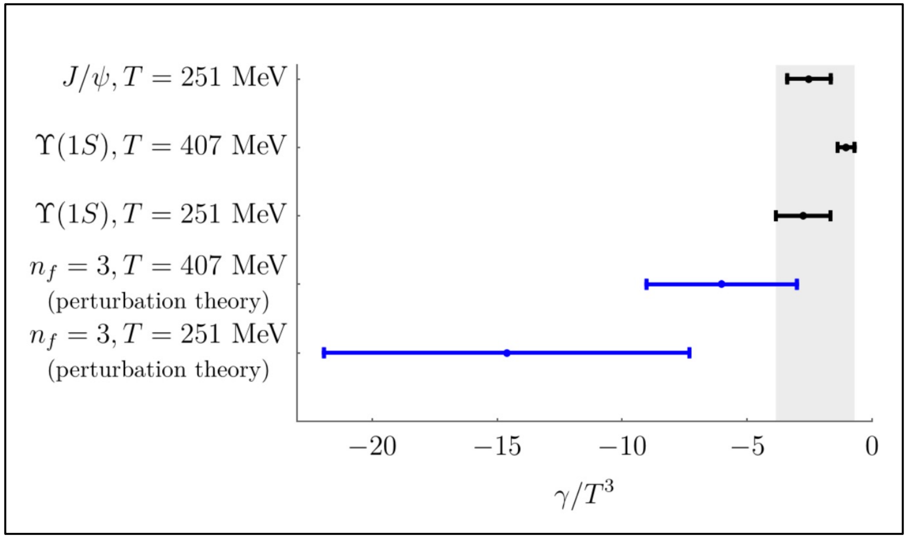

N. Brambilla, M. A. Escobedo, A. Vairo and P. Vander Griend, 1903.08063.

How can one numerically solve these equations?

$$\frac{d\rho_{\rm probe}}{dt} = -iH_{\rm eff}\rho_{\rm probe} + i\rho_{\rm probe}H_{\rm eff}^\dagger + \sum_n C_n\,\rho_{\rm probe}\,C_n^\dagger$$

- Each block of the density matrix in color space can be decomposed into orbital angular momentum blockwise.
- Upon truncating in angular momentum ($l \leq l_{max}$) one can reduce both the singlet and octet blocks of the reduced density matrix to size $(l_{max} + 1)^2$.
- One can then discretize the radial wavefunction (N = # of lattice points) and evolve the reduced density matrix using standard differential equation and matrix solvers gives $\sim N^2(l_{max} + 1)^2$ matrix size.
- **Need to describe bound and unbound states with highly localized initial wave function, so the box must be large and have small lattice spacing → large N and large l_{max}.**
- As N and l_{max} become large, **the computation becomes very challenging**.
- **Need a better/faster method which we can easily parallelize.**

A parallelizable approach: Quantum trajectories

N. Brambilla, M.-A. Escobedo, M.S., A. Vairo, P. Vander Griend, and J.H. Weber, 2012.01240

$$\frac{d\rho_{\rm probe}}{dt} = -iH_{\rm eff}\rho_{\rm probe} + i\rho_{\rm probe}H_{\rm eff}^{\dagger} + \sum_n C_n\, \rho_{\rm probe}\, C_n^{\dagger}$$

Non-unitary "no jump" evolution   Can treat this "quantum jump" term stochastically

- Can be reduced to the solution of a large set of "quantum trajectories" in which we solve a 1D Schrödinger equation with a **non-Hermitian Hamiltonian $\boldsymbol{H_{\rm eff}}$**, subject to **stochastic quantum jumps**.
- The evolution with the non-Hermitian $H_{\rm eff}$ preserves the color and angular momentum state of the system (but not norm).
- Collapse/jump operators encode transitions between different color/angular momentum states (subject to selection rules).

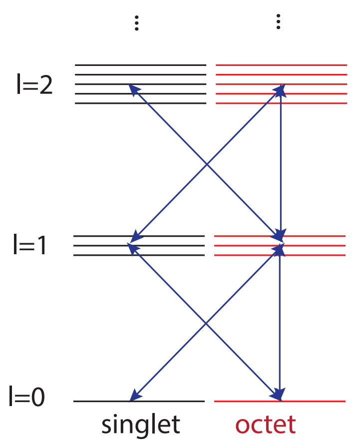

- For each **physical trajectory** (path through the QGP) we average over a large set of **<u>independent</u> quantum trajectories** → **Embarrassingly parallel**
- **Added benefit: Can describe all angular momentum states (no cutoff) .**

Initial bottomonium wavefunction

- We took the initial wavefunction to be given by a smeared delta function (local production due to large mass, Δ ~ 1/M) of the form

$$u_\ell(r, \tau = 0) \propto r^{\ell+1} \exp(-r^2/\Delta^2)$$

- For a given l, the **initial state is a quantum linear superposition** of the eigenstates of H.
- **Includes both bound and unbound states.**
- We took $\Delta = 0.2\ a_0$ which reproduces results obtained with a true delta to within 1%.

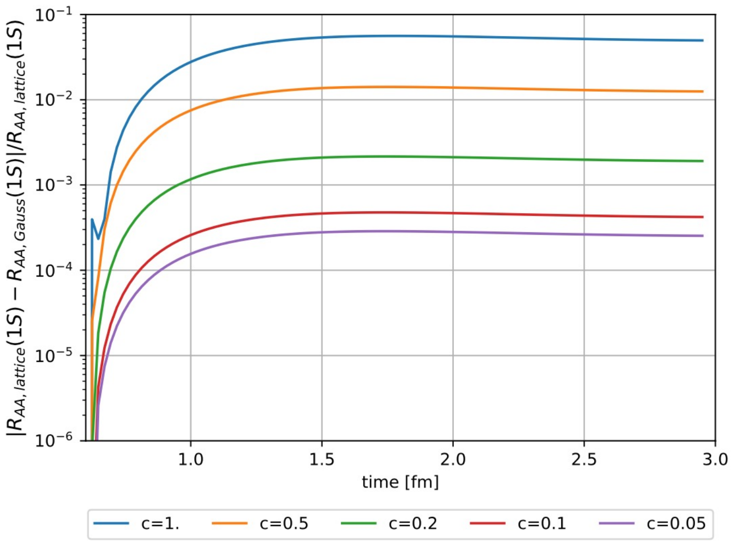

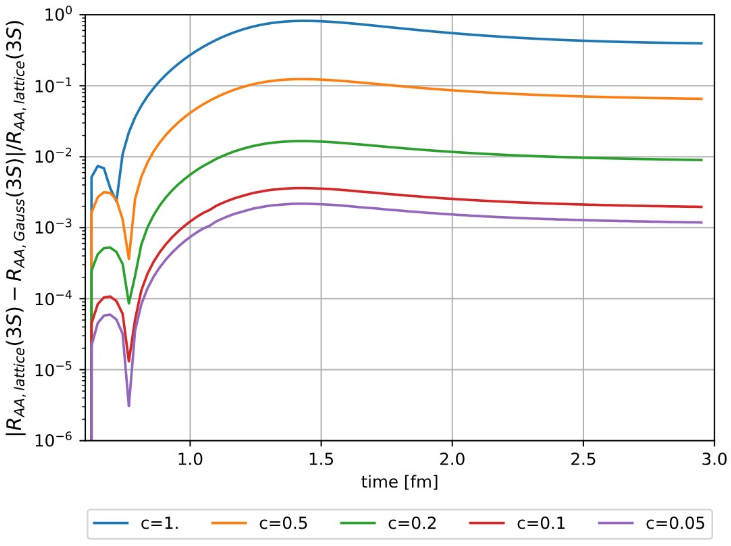

Computing survival probabilities with QTraj

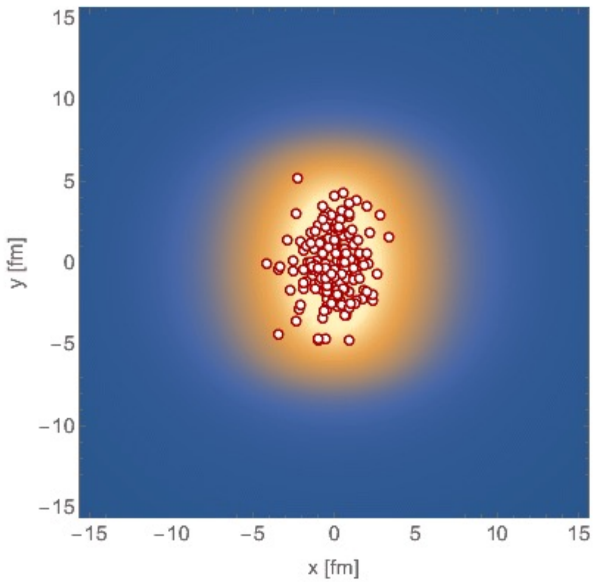

Survival probability

$$SP(n,l) = \frac{|\langle n,l|\psi(t_f)\rangle|^2}{|\langle n,l|\psi(t_0)\rangle|^2}$$

- Used $N = 4096$ lattices
- $L = 108\ a_0$
- $\Delta t = 2 \times 10^{-4}$ fm

- We sampled bottomonium production points and transverse momentum using Monte Carlo sampling.
- 4D temperature profiles provided by 3+1D anisotropic hydrodynamics (very good description of identified hadron spectra and flow).
- We solved the real-time Schrödinger equation with a complex potential and stochastically sampled jumps → Lindblad equation.
- We then solved for the survival probability for S- and P-wave states (see box to the left).
- **For the results reported today, we used 700-900k physical trajectories for each value of the model parameters (35 million total when including average over quantum trajectories).**

Feed-down implementation

$$\vec{N}_{\rm observed} = F \vec{N}_{\rm direct}$$

$$F = \begin{pmatrix} 1 & 0.2645 & 0.0194 & 0.352 & 0.18 & 0.0657 & 0.0038 & 0.1153 & 0.077 \\ 0 & 1 & 0 & 0 & 0 & 0.106 & 0.0138 & 0.181 & 0.089 \\ 0 & 0 & 1 & 0 & 0 & 0 & 0 & 0 & 0 \\ 0 & 0 & 0 & 1 & 0 & 0 & 0 & 0.0091 & 0 \\ 0 & 0 & 0 & 0 & 1 & 0 & 0 & 0 & 0.0051 \\ 0 & 0 & 0 & 0 & 0 & 1 & 0 & 0 & 0 \\ 0 & 0 & 0 & 0 & 0 & 0 & 1 & 0 & 0 \\ 0 & 0 & 0 & 0 & 0 & 0 & 0 & 1 & 0 \\ 0 & 0 & 0 & 0 & 0 & 0 & 0 & 0 & 1 \end{pmatrix}$$

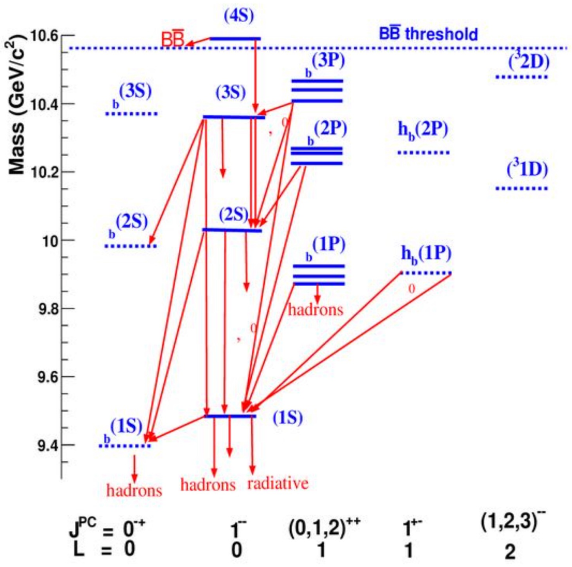

- N_{direct} corresponds to $(N_{1S}, N_{2S}, N_{1P} \times 3, N_{3S}, N_{2P} \times 3, N_{2D})^T$ where, e.g., N_{1S} is the final number of Y(1S) states that can decay in the dilepton channel.

- N_{direct} can be obtained using $<N_{bin}(b)>$ * σ_{direct} * (Survival probability)

- After feed down, we then normalize to by the pp collision result scaled to AA → R_{AA}.

$$R^i_{AA}(c) = \frac{(F \cdot S(c) \cdot \vec{\sigma}_{\rm direct})^i}{\sigma^i_{\rm exp}}$$

OQS+pNRQCD predictions for R_{AA} vs N_{part}

N. Brambilla, M.-A. Escobedo, M.S., A. Vairo, P. Vander Griend, and J.H. Weber, forthcoming

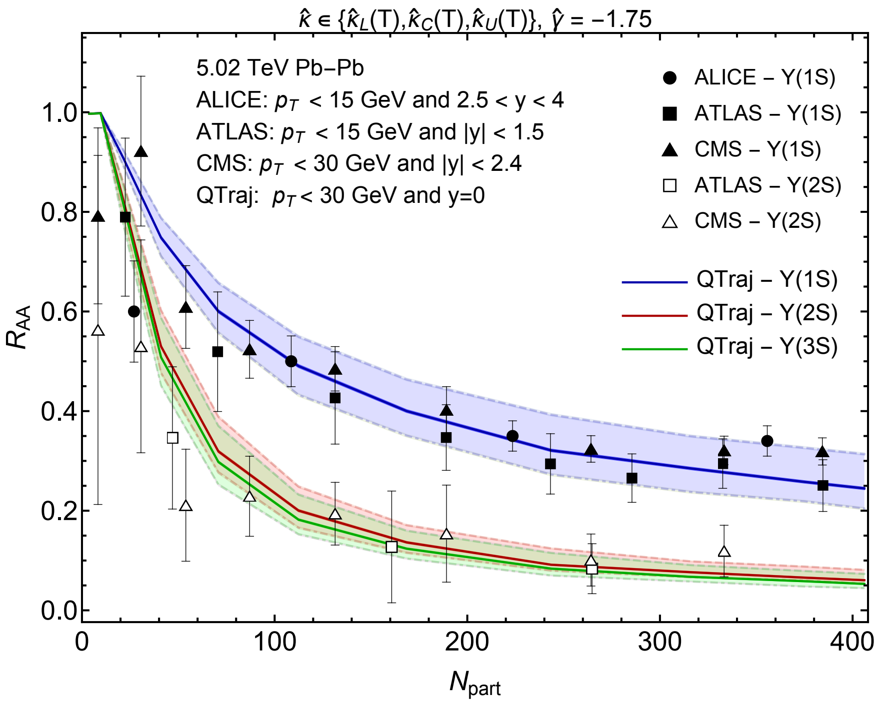

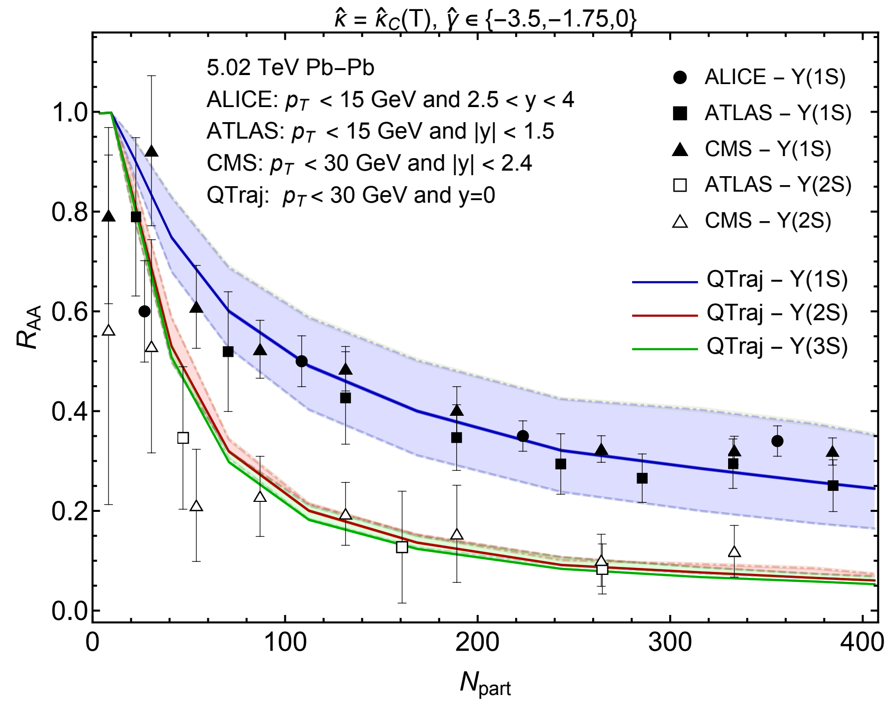

- **Left panel**: Result including feed down, when varying $\hat{\kappa}$ over the theoretical uncertainty.
- **Right panel**: Result including feed down, when varying $\hat{\gamma}$ over the theoretical uncertainty
- Statistical uncertainty associated with average over trajectories is on the order of the line width.

Effects of quantum jumps

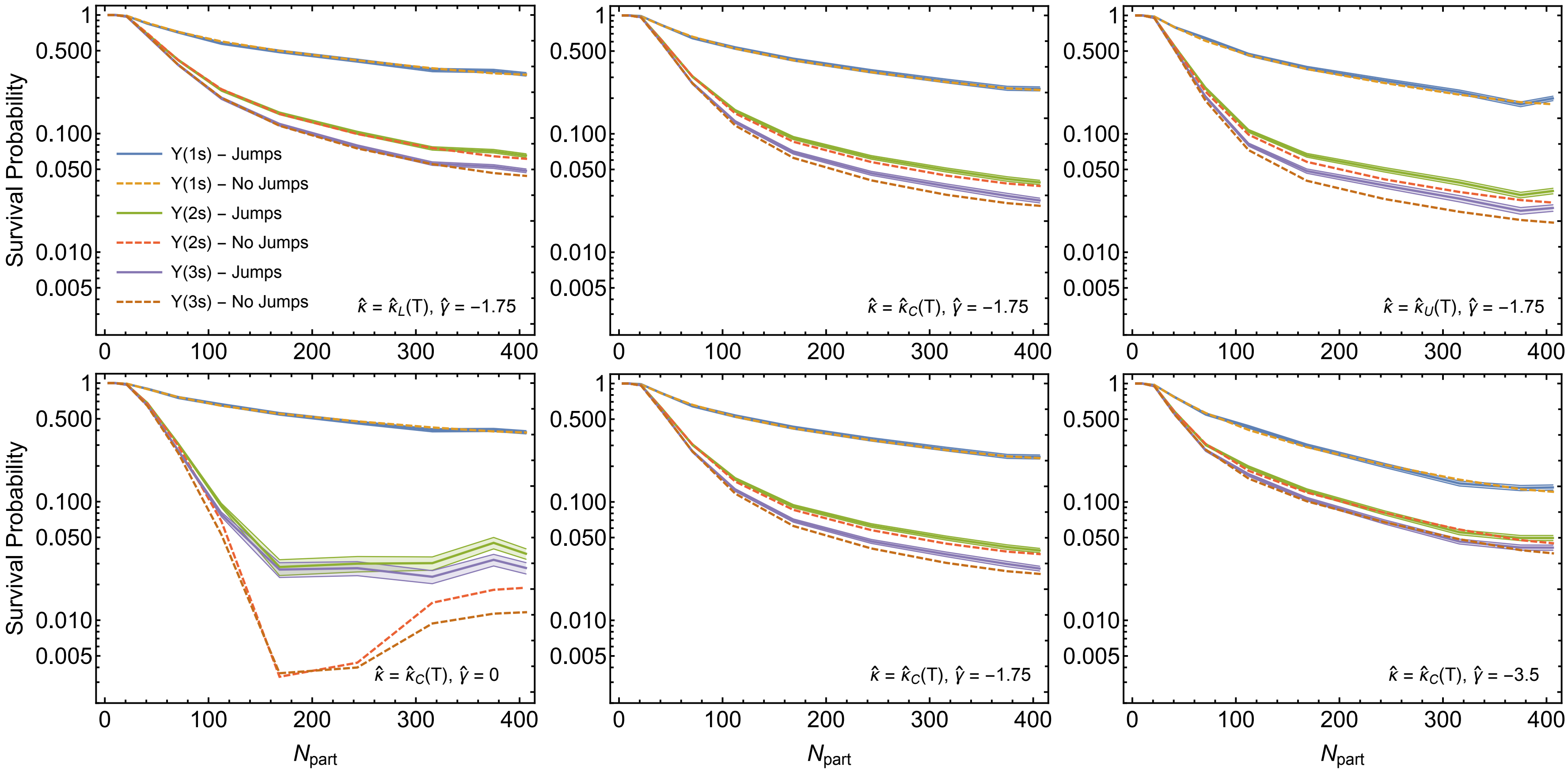

- **Solid lines show result with jumps**
- **Dashed lines show result without jumps (H_{eff} evolution)**

2S/1S and 3S/1S double ratios

N. Brambilla, M.-A. Escobedo, M.S., A. Vairo, P. Vander Griend, and J.H. Weber, forthcoming

2S/1S

3S/1S

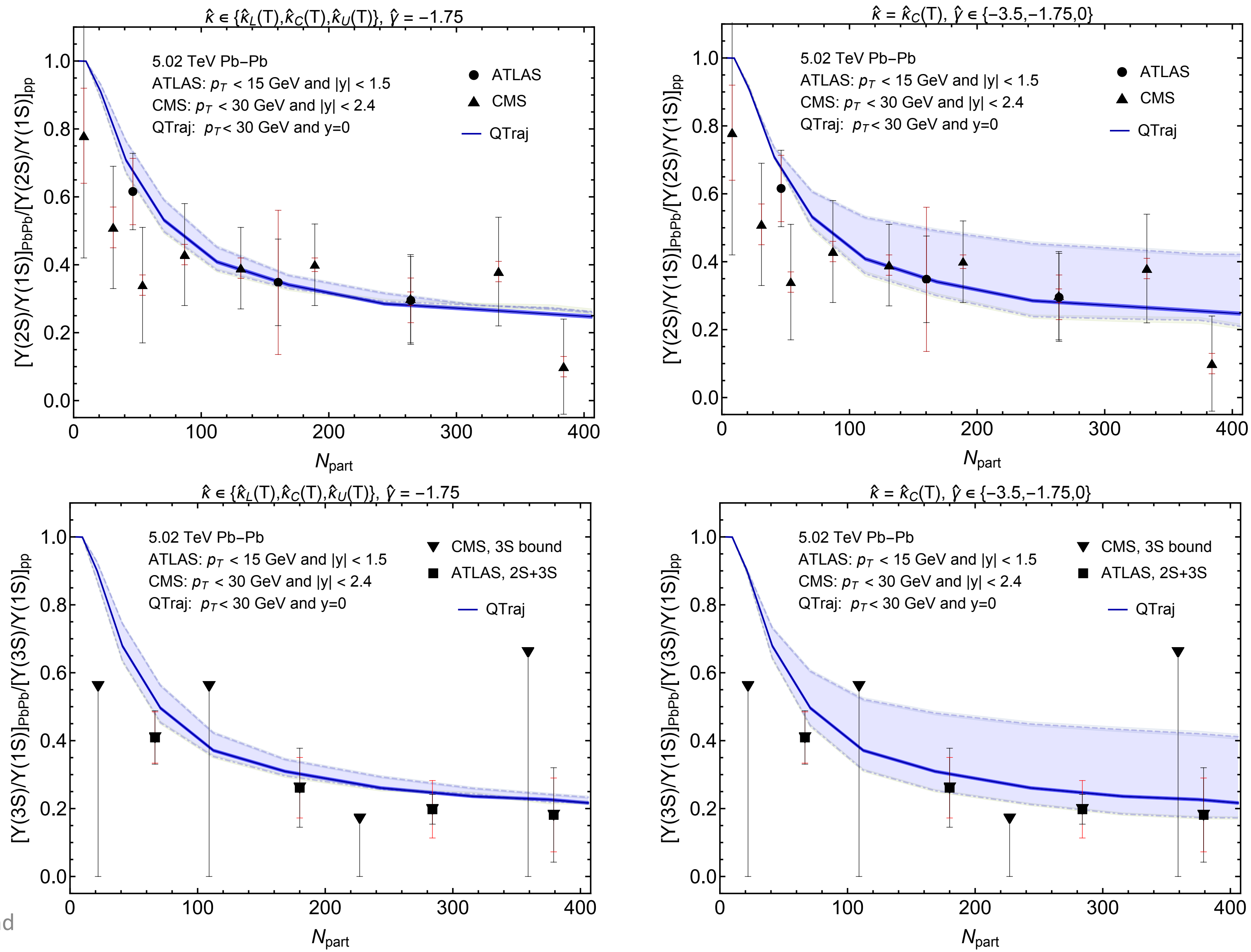

2S/1S ratio vs transverse momentum

N. Brambilla, M.-A. Escobedo, M.S., A. Vairo, P. Vander Griend, and J.H. Weber, forthcoming

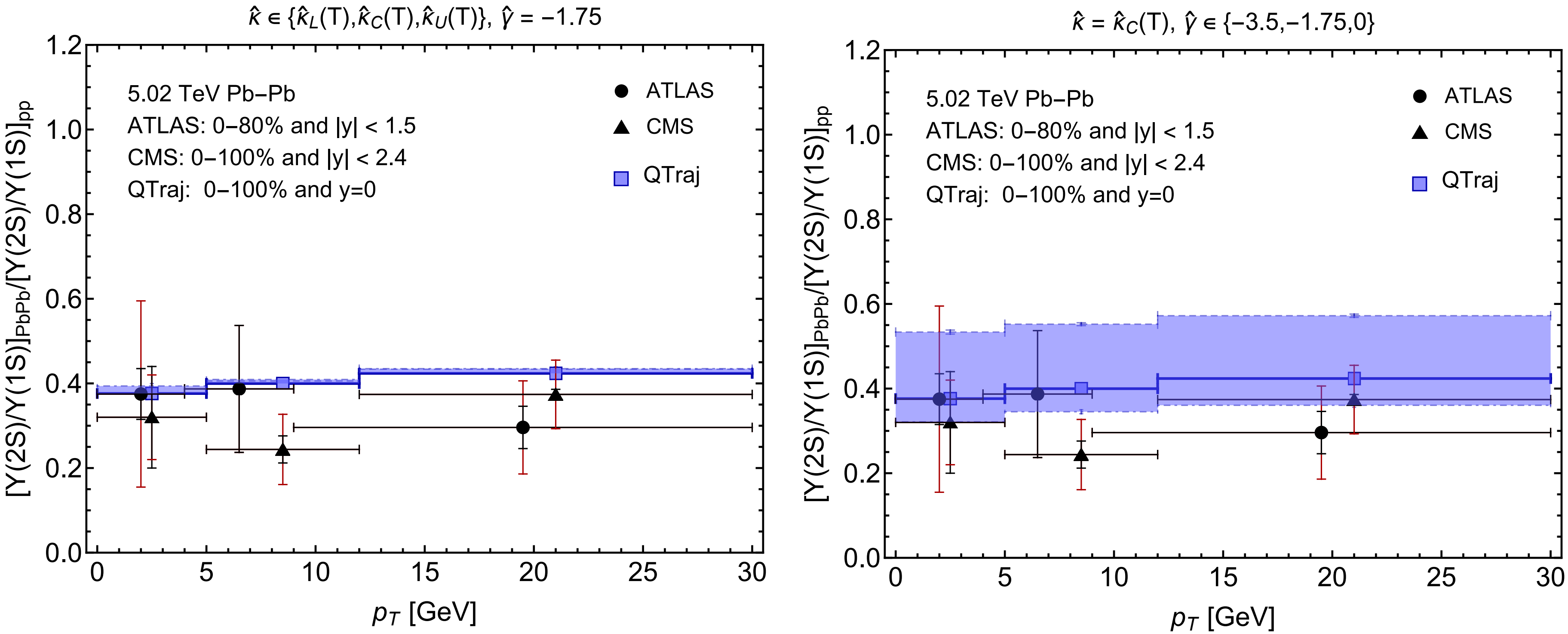

- Result does not depend on choice of κ, however, we see larger variation when varying γ; **value of $\gamma = -3.5$ has tension with data**

- **This offers some hope to constrain this parameter from the 2S/1S double ratio**

Momentum-space anisotropies

4d flow tomography

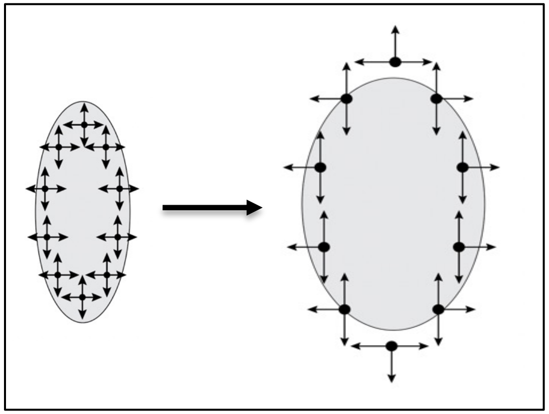

- Bottomonium don't flow in the "collective flow" sense.
- However, there are momentum-space anisotropies induced by path-length differences along the short and long sides of the QGP.

Cern Courier, Fall 2019

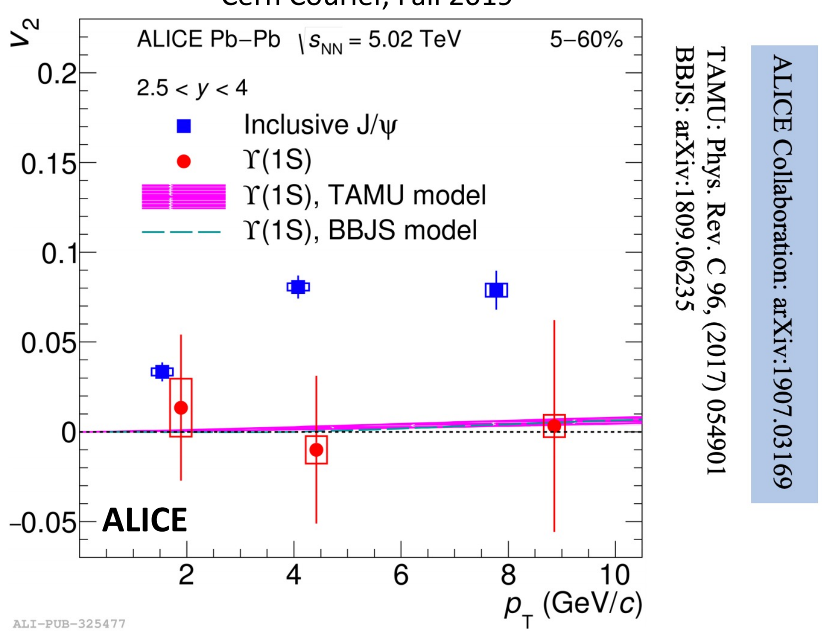

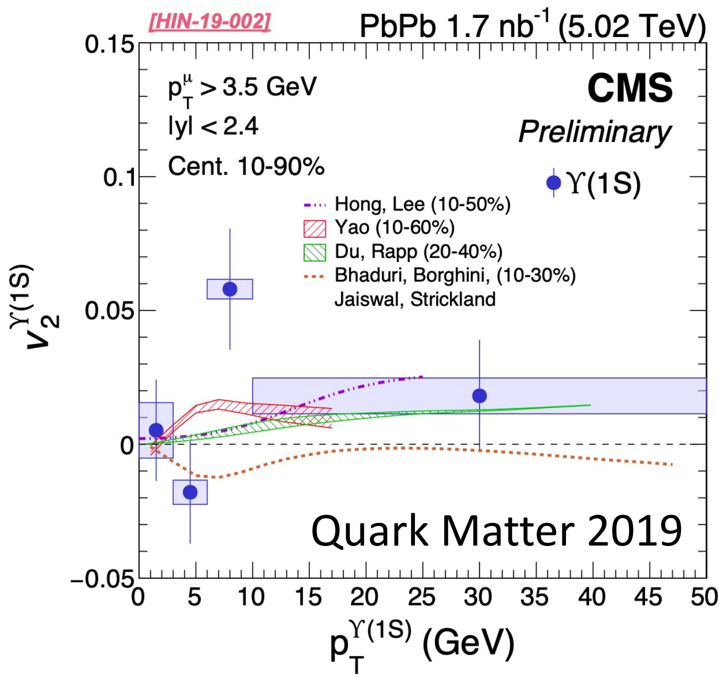

Momentum-space anisotropies

N. Brambilla, M.-A. Escobedo, M.S., A. Vairo, P. Vander Griend, and J.H. Weber, forthcoming

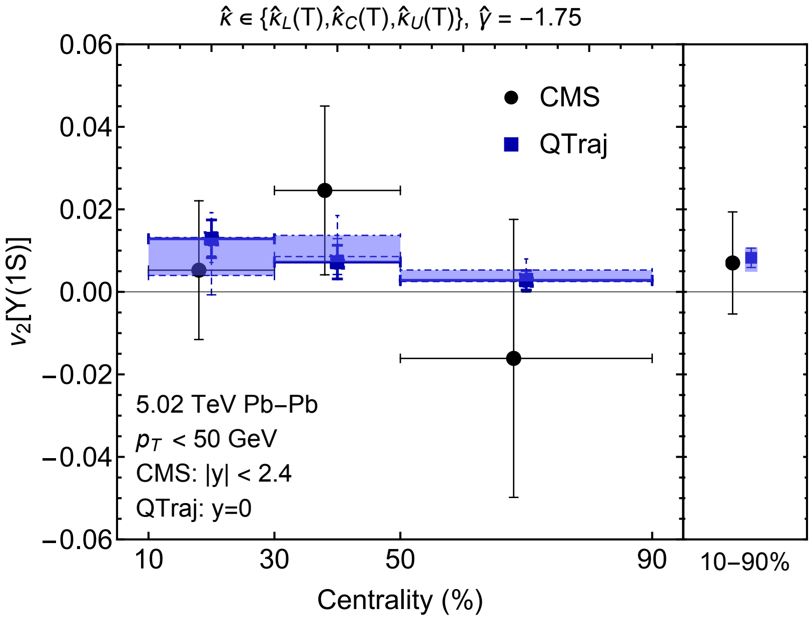

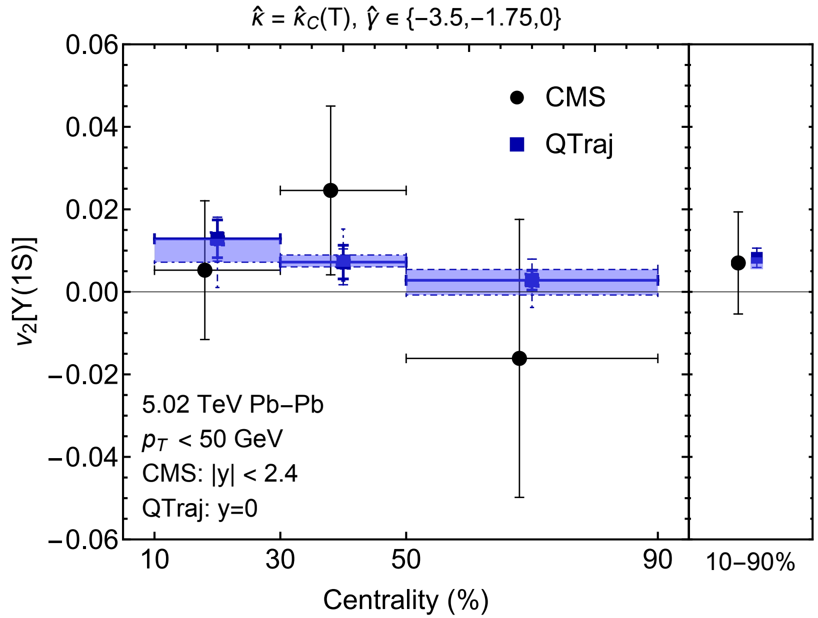

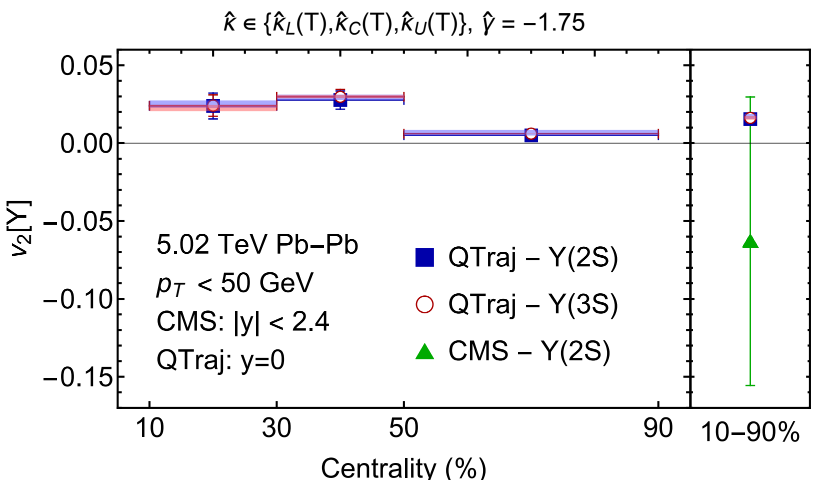

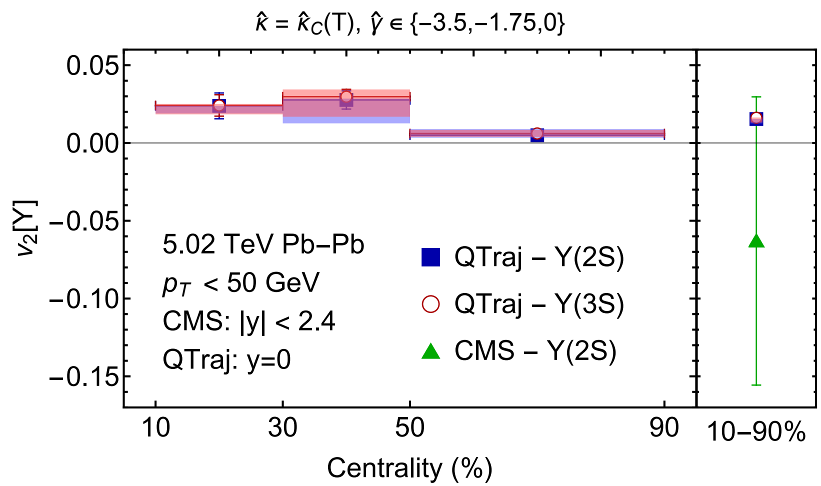

Momentum-space anisotropies

N. Brambilla, M.-A. Escobedo, M.S., A. Vairo, P. Vander Griend, and J.H. Weber, forthcoming

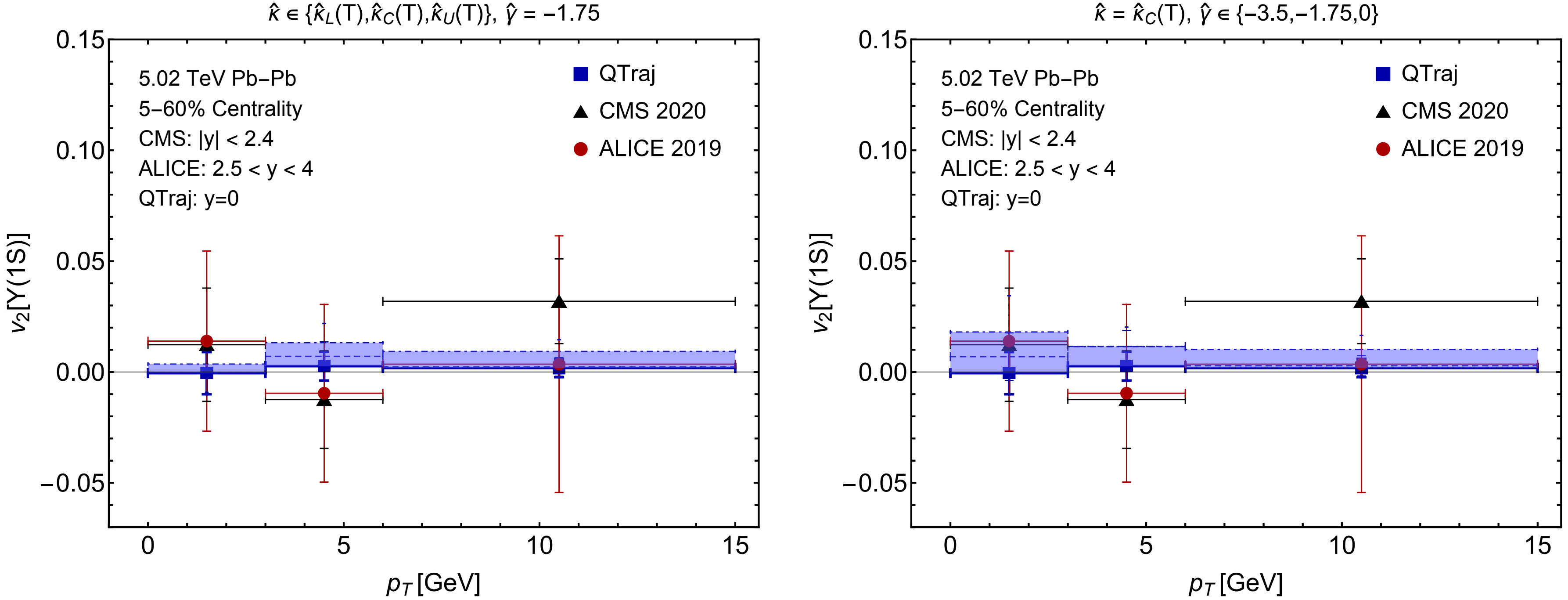

- Υ(1S) v_2 due to path length differences in suppression is small.
- Qtraj predicts $|v_2[\Upsilon(1s)]| < 0.02$ at all p_T.
- Magnitude is consistent with prior works.
- Data have large uncertainties, hopefully more statistics in the future.

Conclusions and Outlook

- OQS + pNRQCD approach works very well to describe the suppression vs N_{part} and p_T, double ratios, and "flow" seen at LHC.
- **First fully quantum and non-abelian treatment of OQS in QGP.**
- Transport coefficients used were **constrained by independent lattice measurements**.
- Demonstrated that Upsilon R_{AA} and double ratios can be used to provide **experimental constraints on these transport coefficients**.
- The **quantum trajectory algorithm** (implemented in QTraj) allowed us to **include effect of quantum jumps between color and angular momentum states in a computationally scalable manner**.
- One outstanding issue is the transition to low-temperature bottomonium dynamics ($T < 200 - 250\ \text{MeV}$). Different ordering of scales, no longer an imaginary part at leading order in the power counting, E/T corrections needed → **work in progress**.

Additional slides

Dependence on T_f

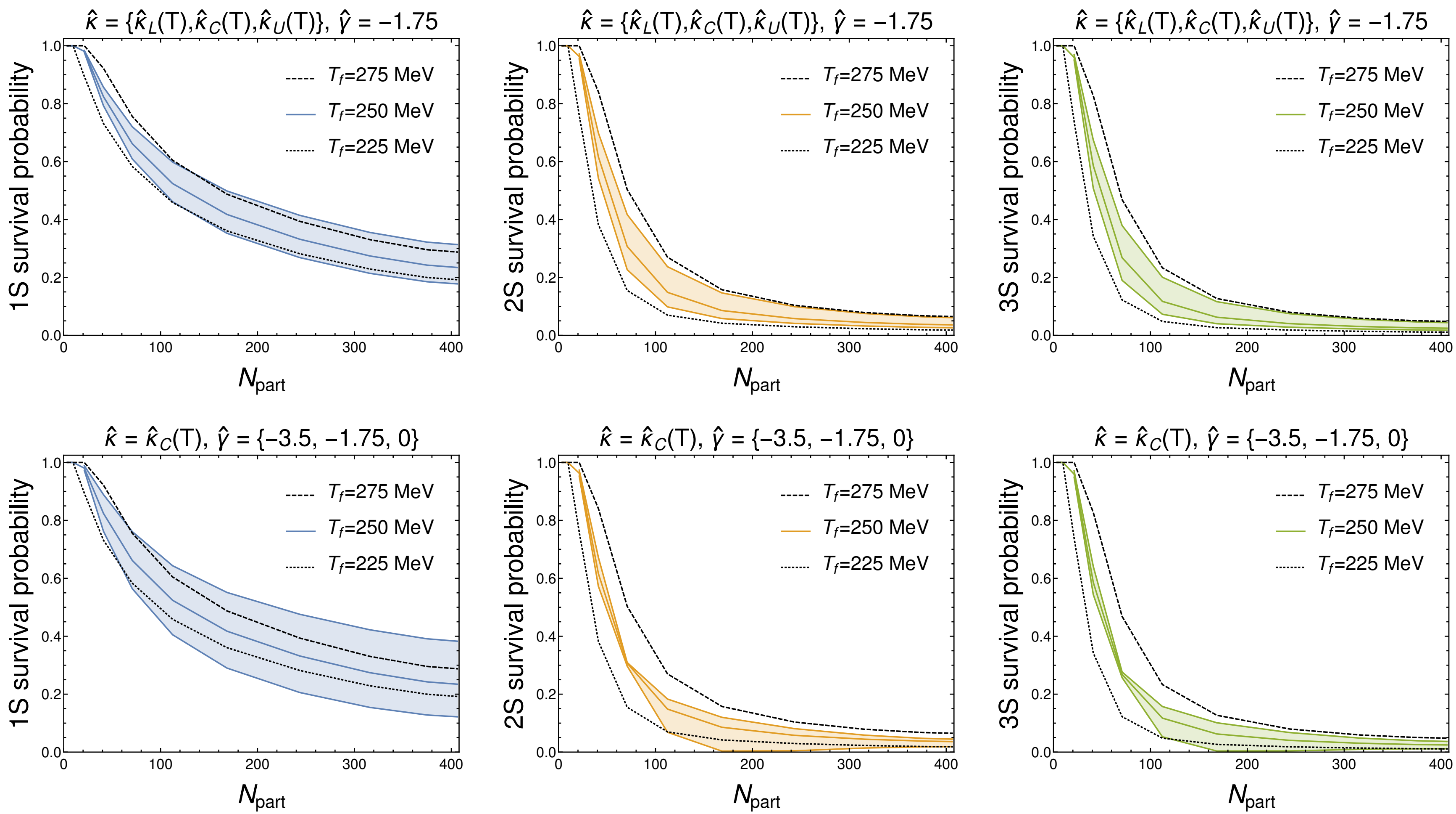

3+1D hydrodynamical background

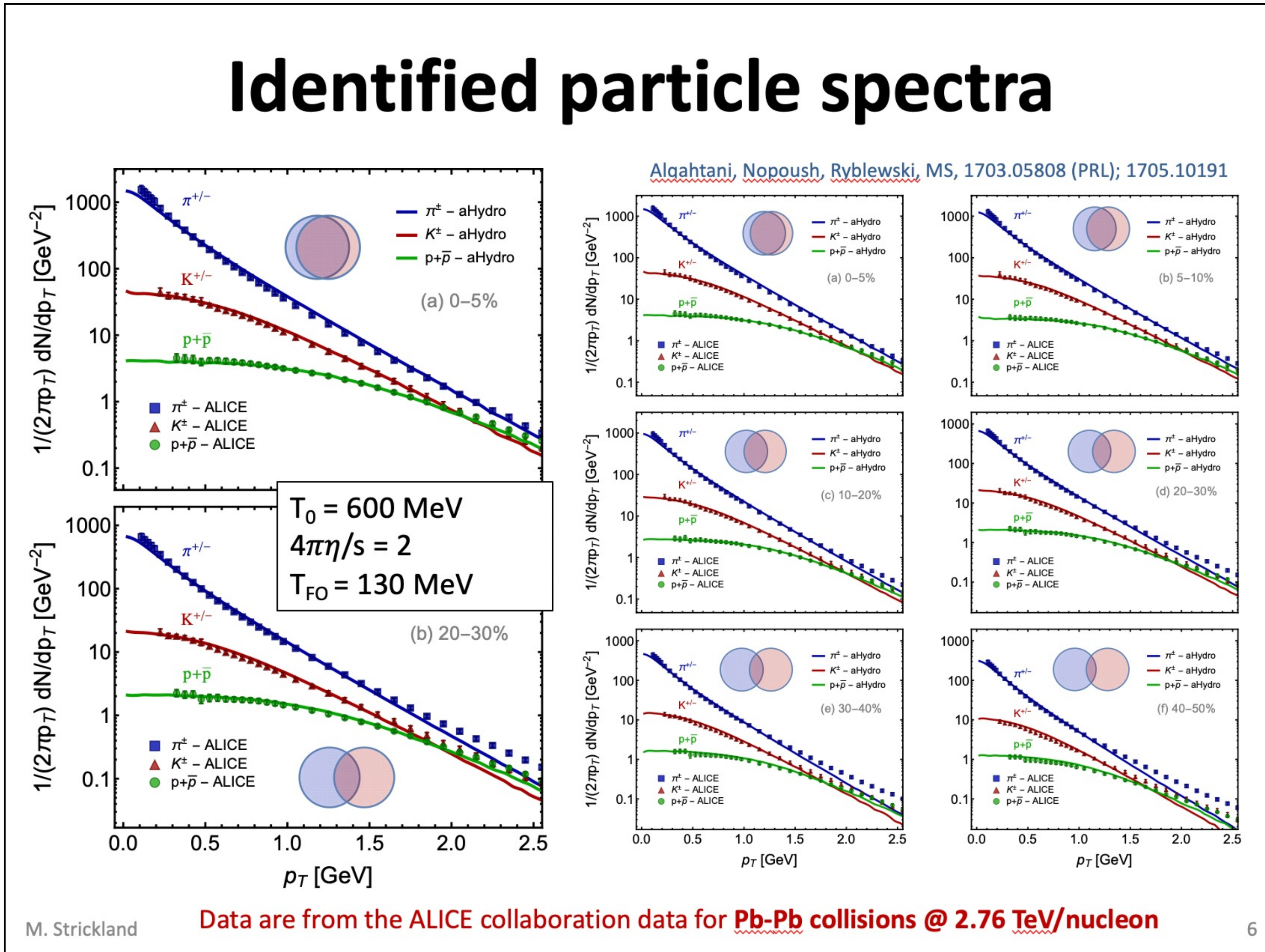

- We use a 3+1D dissipative code for the hydro background (quasiparticle anisotropic hydrodynamics)
- Has been tuned to RHIC and LHC heavy ion collisions
- Reproduces spectra, multiplicities, identified elliptic flow of light hadrons, HBT radii, etc.

For 5.02 TeV, T_0 = 630 MeV @ t_0 = 0.25 fm/c